ACADEMIC PRESS

Available online at www.sciencedirect.com

SCIENCE DIRECT®

Journal of Computational Physics 186 (2003) 361–396

JOURNAL OF COMPUTATIONAL PHYSICS

www.elsevier.com/locate/jcp

Discrete equations for physical and numerical compressible multiphase mixtures

Rémi Abgrall [a,*,1], Richard Saurel [b,2]

[a] *Institut Universitaire de France and Université de Bordeaux I, Département de Mathématiques Appliquées, 351 cours de la Libération, 33405 Talence, France*

[b] *Institut Universitaire de France and Polytech'Marseille, IUSTI, 5 rue Enrico Fermi, 13453 Marseille Cedex 13, France*

Received 4 July 2002; received in revised form 21 November 2002; accepted 24 December 2002

Abstract

We have recently proposed, in [21], a compressible two-phase unconditionally hyperbolic model able to deal with a wide range of applications: interfaces between compressible materials, shock waves in condensed multiphase mixtures, homogeneous two-phase flows (bubbly and droplet flows) and cavitation in liquids. One of the difficulties of the model, as always in this type of physical problems, was the occurrence of non-conservative products. In [21], we have proposed a discretisation technique that was without any ambiguity only in the case of material interfaces, not in the case of shock waves. This model was extended to several space dimensions in [24], In this paper, thanks to a deeper analysis of the model, we propose a class of schemes that are able to converge to the correct solution even when shock waves interact with volume fraction discontinuities. This analysis provides a more accurate estimate of closure terms, but also an accurate resolution method for the conservative fluxes as well as non-conservative terms even for situations involving discontinuous solutions. The accuracy of the model and method is clearly demonstrated on a sequence of difficult test problems.

Keywords: Multiphase flows; Compressible flows; Godunov schemes; Non-conservative systems

1. Introduction

Multiphase flows are involved in a huge amount of fundamental and industrial applications while multiphase mixtures may have several origins. Usually they are consequences of a physical mixing process of several fluids or materials. But in some circumstances, they may come from artificial (numerical)

* Corresponding author. Fax: +33-5-56-84-26-26.
E-mail addresses: remi.abgrall@math.u-bordeaux.fr (R. Abgrall), richard.saurel@polytech.univ-mrs.fr (R. Saurel).
[1] Also INRIA Projet Scalapplix.
[2] Also, INRIA Projet SMASH.

0021-9991/03/$ - see front matter
doi:10.1016/S0021-9991(03)00011-1

smearing of contact discontinuities separating fluids of different physical and chemical properties, this is what we call numerical mixtures.

In this paper, we are interested in the numerical approximation of compressible inviscid multiphase flows. Although we are aware that viscous terms and turbulence can be omitted only in very special situations, this is nevertheless, from a numerical point of view, a fundamental situation. If one is interested in the simulation of compressible viscous or turbulent multiphase flows, one of the building block of the numerical scheme is nevertheless the scheme aimed at the approximation of the convective and acoustic phenomena; this is precisely the topic of this paper.

In a previous work [21], we have proposed an unconditionally hyperbolic model able to deal with physical mixtures as well as with numerical ones. It is written as a sum of conservative and non-conservative product terms, complemented with pressure and velocity relaxation terms, which, as explained in this reference, modelise micro-scale phenomena. The model of [21] is another interpretation of the Baer and Nunziato [3] model for wave propagation in compressible mixtures. In the same reference, a new numerical method able to deal with compressible mixtures, as well as interface problems, was developed.

However, the model and the method of [21] were suffering of some imperfections:

- The closure laws for the average interfacial velocity and pressure were left unclear. This is not surprising because there is no known solution to this closure problem. It is usually considered as mixture topology dependent and is one of the major issue in two-phase flows modeling. However, the choices we made were not really important for the applications we considered.
- The approximation of the non-conservative terms, involving the volume fraction gradient, the interface pressure and velocity, was carefully done for contact discontinuities, but was left unclear for shock interaction with volume fraction discontinuities.

The question of how to discretise the non-conservative terms occurring in two-phase flow problems has already been addressed by many authors including [3,4,8,9,13,15], etc. In [13], these terms were canceled, thus eliminating the difficulty. In [3,4,8,9,13,15] the shock relations are derived without considering any variation of the volume fraction at shock front. The volume fraction is evolving with the convective velocity (gas or solid velocity or velocity of the mixture) which is different of the shock velocity. Indeed, if the analysis is conducted with the hyperbolic system without relaxation terms, the result seems plausible. But physical situations always involve relaxation terms which are the trace of micro-scale phenomena, such as bubble expansion or compression. These relaxation terms involve volume variations inside the shock front, hence there are some difficulties to determine rigorously shock relations, and of course the associated numerical approximations. Moreover, there are physical situations where volume fraction varies across shock front due to mass transfer : detonation, cavitation and condensation problems. In this paper, we also show that these relaxation terms have a direct connection to non-conservative ones, thus they cannot be omitted. In fact, we show that part of the non-conservative terms are relaxation terms.

In most models for two-phase flows, the system of PDEs is not written in conservative form. This results in difficult numerical and mathematical problems because discontinuous solutions have to be considered, and a rigorous definition of weak solutions needs to be given. This is a necessary step to correctly approximate the non-conservative terms in the system. This problem has motivated many researchers, see for example [5,19,26]. For example, Sainsaulieu proposes to introduce additional viscous effects in order to regularise the solution, and seek for the limit solution when the viscosity parameter tends to zero. This program is complex and can only be conducted until the end only in special situations [20]. The solution to this problem is of fundamental importance because numerical solution may be very sensitive to the treatment of non-conservative products [14].

We believe that the existence of non-conservative terms is a result of multidimensional motion at the flow micro-scales, rather than a viscous process. Imagine two fluids inside a tube separated by an interface. The liquid is at the lower part of the tube, while the gas is at the upper part. The column is impacted by a high velocity piston on its left side as depicted in Fig. 1. Since the two fluids are considered as compressible, there

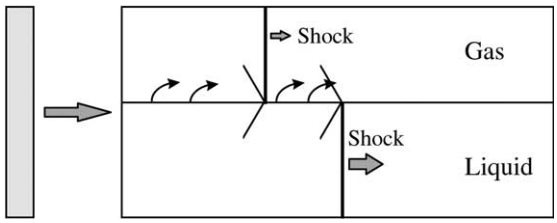

Fig. 1. Schematic representation of shock waves propagation in a separated two-phase mixture.

are two shock waves propagating in the liquid and in the gas. Since each fluid has its own physical properties and equations of state, the shock waves have two distinct velocities. A consequence is that the post-shock pressure is different in the two phases, even if they were originally equal. The variation in the post-shock pressure must be "relaxed" because the gas and liquid pressure must be equal across the slip line that separates them. This is obtained via transverse waves that propagates in the gas and the liquid so that the pressures tend to equilibrate across the slip line. During this relaxation process, the interface moves with a two- or three-dimensional motion. After the transverse waves propagation, the two shock waves collapse on a single two-dimensional complicated wave for the configuration represented in Fig. 1. We note that the velocity is not continuous across the slip line, only its normal component is.

A two-dimensional direct numerical simulation of this problem is done in Fig. 2 with the numerical scheme described in [22] which is particularly adapted to interface problems. When the mixture contains bubbles, droplets, or any density discontinuity, similar hydrodynamic process occurs at the scale of individual particles, thus this simulation can be seen as the simulation in a small volume surrounding a bubble interface. Such type of process does not involve fluid viscosity. From these two figures it is clear that the volume fraction varies inside the shock because the volume of the phases cannot stay constant when a pressure difference exists.

The wave-like structure one can observe at a macroscopic scale is obtained by homogenisation of such micro-scales problems. The model and method developed in [21] addresses the problem of micro-scale motion by introducing relaxation parameters for pressure and velocity. These relaxation terms are summarising the sum of multidimensional micro-scale motions.

A first implementation of this remark is done in [21]. The non-conservative terms were considered and physically based discretisations of them are proposed. The numerical approximations are derived by

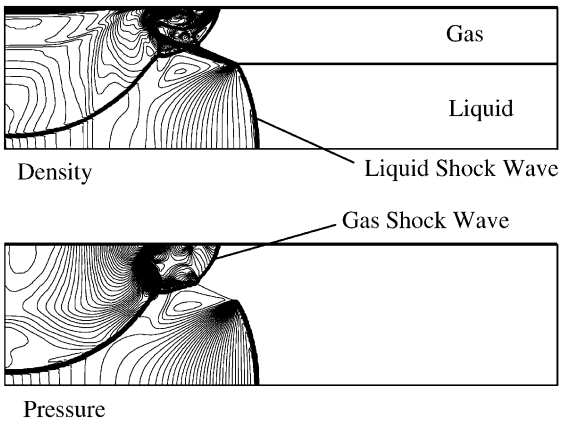

Fig. 2. Numerical simulation of shock propagation in separated two-phase mixtures. Density and pressure contours.

considering a flow with a uniform velocity and pressure; the idea is to keep such wave structure invariant by the scheme. Such approximations are valid for interfaces because the volume fraction, and not the velocity and pressure, may be discontinuous: the situation is much simpler than for shock waves.

In this paper, we proceed in the opposite way to what is done usually. Usually, the multiphase flow equations are considered at the continuous level and are then approximated by a numerical method. Here, we consider the pure phase Euler equations at the microscopic level. We give numerical approximations of these equations in the context of interface problem at the micro-scale via the Godunov scheme [12]. These approximations are then averaged over the set of all possible realisations and provide the corresponding scheme for the averaged multiphase flow equations. We provide the detailed form of each term.

The corresponding scheme is applied to severe test problems and shows a perfect accuracy with respect to the exact solution when it is known. The method behaves perfectly with interface problems as well as with physical mixtures.

The paper is organised as follows. First, we recall the averaging technique developed in Drew and Passman [7] when ensemble average is used. Our numerical scheme is derived by imitating, at the discrete level, the averaging method of Drew and Passman. We then show how to derive high order extension of the scheme. The efficiency of the method is demonstrated on several conventional and other difficult test cases.

2. Preliminaries

2.1. Derivation of the continuous PDEs

We first recall the method to obtain the compressible multiphase model. The dissipative effects and phase changes are not considered in the present work. Here, we assume that for each realization, the interface between the phases is well defined; in particular it is possible to define, for any physical points located on the interface, an interface velocity. It is the velocity at which the interface locally moves.

We consider the case of two phases Σ_1 and Σ_2. Each pure fluid is governed by the Euler equations

$$\frac{\partial U^{(k)}}{\partial t} + \nabla \cdot F^{(k)} = 0, \quad k = 1, 2. \tag{1}$$

In (1), we set $U^{(k)} = (\rho^{(k)},\ \rho^{(k)}\mathbf{u}^{(k)},\ \rho^{(k)}E^{(k)})^{\mathrm{T}}$ and $F^{(k)} = (\rho^{(k)},\ \mathbf{u}^{(k)},\ \rho^{(k)},\ \mathbf{u}^{(k)} \otimes \mathbf{u}^{(k)} + P^{(k)}Id,\ (\rho^{(k)}E^{(k)} + P^{(k)})\mathbf{u}^{(k)})^{\mathrm{T}}$, where $\rho^{(k)}$ is the density, $u^{(k)}$ is the velocity, $E^{(k)}$ is the specific energy ($E^{(k)} = e^{(k)} + 1/2\mathbf{u}^{(k)} \cdot \mathbf{u}^{(k)}$, where $e^{(k)}$ is the internal energy) and $P^{(k)}$ is the pressure of phase Σ_k. We assume that each pure phase admits a convex equation of state $P^{(k)} = P^{(k)}(e^{(k)}, \rho^{(k)})$.

We introduce, as in [7], the characteristic function $X^{(k)}$ of phase Σ_k: $X^{(k)}(x,t) = 1$ if x lies in fluid Σ_k at time t, and 0 otherwise. The function $X^{(k)}$ satisfies the topological equation

$$\frac{\partial X^{(k)}}{\partial t} + \sigma \cdot \nabla X^{(k)} = 0, \tag{2}$$

where σ is the interface velocity between the two phases. This equation can be understood by looking at the two cases: either a point is inside one phase or it is at the interface of the two phases. If we look at a point that is not on the interface, either $X^{(k)} = 0$ or 1. In either case, the partial derivatives both vanish, and then the left-hand side of the equation vanishes whatever σ. If the point is on an interface, it moves with the interface velocity, so σ is the interface velocity. Of course, (2) is understood in the sense of distributions, as in [7]. This means that, for any regular compactly supported function φ, and for any volume Ω, if we denote by $\Omega^{(k)}$ the subset of Ω contained in the phase Σ_k, we have

$$\int_{\Omega^{(k)}} \frac{\partial \varphi}{\partial t} + \int_{\partial\Omega^{(k)}} \sigma \cdot \mathbf{n}\varphi = 0. \tag{3}$$

In (3), $\mathbf{n}$ is the exterior unit normal to $\Omega^{(k)}$. Eq. (3) reveals that σ is the velocity of the interface between the two phases.

Drew and Passmann [7] consider averaging procedures $\mathscr{E}(\cdot)$ that commute with the time and space derivative. For any function f, we assume

$$\begin{aligned} &\mathscr{E}\left(\frac{\partial f}{\partial t}\right) = \frac{\partial \mathscr{E}(f)}{\partial t}, \\ &\mathscr{E}(\nabla f) = \nabla \mathscr{E}(f) \end{aligned} \tag{4}$$

for which they establish the two calculation rules (see [7, pp. 102–103])

$$\begin{aligned} &\mathscr{E}\left(X^{(k)}\nabla f\right)\mathscr{E}\left(\nabla X^{(k)} f\right) - \mathscr{E}\left(f_{\text{int}}^{(k)} \nabla X^{(k)}\right) \quad \text{Gauss rule,} \\ &\mathscr{E}\left(X^{(k)}\frac{\partial f}{\partial t}\right) = \mathscr{E}\left(\frac{\partial f X^{(k)}}{\partial t}\right) - \mathscr{E}\left(f_{\text{int}}^{(k)}\frac{\partial X^{(k)}}{\partial t}\right) \quad \text{Leibniz rule.} \end{aligned} \tag{5}$$

In (5), f is any function, $f_{\text{int}}^{(k)}$ is the value f at an interface on the component k of the interface: if M is located on an interface between Σ_1 and Σ_2, $f_{\text{int}}^{(k)}$ is the limit value of $f(P)$ when $P \to M$ stays in the phase Σ_k.

Using these rules for $f = X^{(1)}U^{(1)} + x^{(2)}U^{(2)}$ and $f = X^{(1)}F^{(2)} + X^{(2)}F^{(2)}$, we get ([7, pp. 121–122]), the system

$$\begin{aligned} &\frac{\partial \mathscr{E}\left(X^{(k)}\rho^{(k)}\right)}{\partial t} + \nabla \cdot \mathscr{E}\left(X^{(k)}\rho^{(k)}\mathbf{u}^{(k)}\right) = \mathscr{E}\left(\rho^{(k)}\left(\mathbf{u}^{(k)} - \sigma\right) \cdot \nabla X^{(k)}\right), \\ &\frac{\partial \mathscr{E}\left(X^{(k)}\rho^{(k)}\mathbf{u}^{(k)}\right)}{\partial t} + \nabla \cdot \left(\mathscr{E}\left(X^{(k)}\rho^{(k)}\mathbf{u}^{(k)} \otimes \mathbf{u}^{(k)}\right) + \mathscr{E}\left(X^{(k)}P^{(k)}\right)\right) = \mathscr{E}\left(\left(\rho^{(k)}\mathbf{u}^{(k)} \otimes \left(\mathbf{u}^{(k)} - \sigma\right) + P^{(k)}\right) \cdot \nabla X^{(k)}\right), \\ &\frac{\partial \mathscr{E}\left(X^{(k)}\rho^{(k)}E^{(k)}\right)}{\partial t} + \nabla \cdot \mathscr{E}\left(X^{(k)}\rho^{(k)}E^{(k)}\mathbf{u}^{(k)} + X^{(k)}P^{(k)}\mathbf{u}^{(k)}\right) = \mathscr{E}\left(\left(\rho^{(k)}E^{(k)}\left(\mathbf{u}^{(k)} - \sigma\right) + P^{(k)}\mathbf{u}^{(k)}\right) \cdot \nabla X^{(k)}\right). \end{aligned} \tag{6}$$

Defining the volume fraction of Σ_k as $\alpha^{(k)} = \mathscr{E}(X^{(k)})$, the average density as

$$\overline{\rho^{(k)}} = \frac{\mathscr{E}\left(X^{(k)}\rho\right)}{\alpha^{(k)}} = \frac{\mathscr{E}\left(X^{(k)}\rho^{(k)}\right)}{\alpha^{(k)}},$$

the average velocity

$$\bar{\mathbf{u}} = \frac{\mathscr{E}\left(X^{(k)}\rho\mathbf{u}\right)}{\alpha^{(k)}\overline{\rho^{(k)}}} = \frac{\mathscr{E}\left(X^{(k)}\rho^{(k)}u^{(k)}\right)}{\alpha^{(k)}},$$

etc, and dropping the overline symbol for notational convenience, we get the average balance equations for each phase

$$\begin{aligned} &\frac{\partial \alpha^{(k)}\rho^{(k)}}{\partial t} + \nabla \cdot \left[\alpha^{(k)}\rho^{(k)}\mathbf{u}^{(k)}\right] = \mathscr{E}\left(\rho\left(\mathbf{u}^{(k)} - \sigma\right) \cdot \nabla X^{(k)}\right), \\ &\frac{\partial \alpha^{(k)}\rho^{(k)}\mathbf{u}^{(k)}}{\partial t} + \nabla \cdot \left[\alpha^{(k)}\rho^{(k)}\mathbf{u}^{(k)} \otimes \mathbf{u}^{(k)} + \alpha^{(k)}P^{(k)}\right] = \mathscr{E}\left(\left(\rho^{(k)}\mathbf{u}^{(k)} \otimes \left(\mathbf{u}^{(k)} - \sigma\right) + P^{(k)}\right) \cdot \nabla X^{(k)}\right), \\ &\frac{\partial \alpha^{(k)}E^{(k)}}{\partial t} + \nabla \cdot \left[\left(\alpha^{(k)}E^{(k)}\mathbf{u}^{(k)} + \alpha^{(k)}P^{(k)}\mathbf{u}^{(k)}\right]\right. = \mathscr{E}\left(\left(\rho^{(k)}E^{(k)}\left(\mathbf{u}^{(k)} - \sigma\right) + P^{(k)}\mathbf{u}^{(k)}\right) \cdot \nabla X^{(k)}\right) \end{aligned} \tag{7}$$

coupled with the average topological equation

$$\frac{\partial \alpha^{(k)}}{\partial t} + \mathscr{E}\left(\sigma \cdot \nabla X^{(k)}\right) = 0. \tag{8}$$

In the sequel, we set

$$W = (\alpha^{(1)}\rho^{(1)},\ \alpha^{(1)}\rho^{(1)}\mathbf{u}^{(1)},\ \alpha^{(1)}E^{(1)},\ \alpha^{(1)},\ \alpha^{(2)}\rho^{(2)},\ \alpha^{(2)}\rho^{(2)}\mathbf{u}^{(2)},\ \alpha^{(2)}E^{(2)},\ \alpha^{(2)})^{\mathrm{T}} \tag{9}$$

and

$$\begin{aligned}\mathscr{F}(W) = (&\alpha^{(1)}\rho^{(1)}\mathbf{u}^{(1)},\ \alpha^{(1)}\rho^{(1)}\mathbf{u}^{(1)} \otimes \mathbf{u}^{(1)} + \alpha^{(1)}P^{(1)},\ \alpha^{(1)}(E^{(1)} + P^{(1)})\mathbf{u}^{(1)},\\ &0,\ \alpha^{(2)}\rho^{(2)}\mathbf{u}^{(2)},\ \alpha^{(2)}\rho^{(2)}\mathbf{u}^{(2)} \otimes \mathbf{u}^{(2)} + \alpha^{(2)}P^{(2)},\ \alpha^{(2)}(E^{(2)} + P^{(2)})\mathbf{u}^{(2)},\ 0)^{\mathrm{T}}.\end{aligned} \tag{10}$$

Following one more time Drew and Passman, the weak formulation of (7) is, for any C^1 compactly supported function φ,

$$\int_0^\infty \int_{\mathbb{R}} \left(\frac{\partial \varphi}{\partial t} W + \frac{\partial \varphi}{\partial x} \mathscr{F}(W) \right) - \int_{-\infty}^{\infty} \varphi(x,0) W(x,0)\, \mathrm{d}x = \int_0^\infty \int_{-\infty}^{\infty} \mathscr{E}(\varphi \mathscr{G})\, \mathrm{d}x\, \mathrm{d}t, \tag{11}$$

where

$$\begin{aligned}\mathscr{G} = (&\rho^{(1)}(\mathbf{u}^{(1)} - \sigma) \cdot \nabla X^{(1)},\ (\rho^{(1)}\mathbf{u}^{(1)} \otimes (\mathbf{u}^{(1)} - \sigma) + P^{(1)}) \cdot \nabla X^{(1)},\ (\rho^{(1)}E^{(1)}(\mathbf{u}^{(1)} - \sigma) + P^{(1)}\mathbf{u}^{(1)}) \cdot \nabla X^{(1)},\\ &\sigma \cdot \nabla X^{(1)},\ (\rho^{(2)}(\mathbf{u}^{(2)} - \sigma)) \cdot \nabla X^{(2)},\ (\rho^{(2)}\mathbf{u}^{(2)} \otimes (\mathbf{u}^{(2)} - \sigma) + P^{(2)}) \cdot \nabla X^{(2)},\\ &(\rho^{(2)}E^{(2)}(\mathbf{u}^{(2)} - \sigma) + P^{(2)}\mathbf{u}^{(2)}) \cdot \nabla X^{(2)},\ \sigma \cdot \nabla X^{(2)})^{\mathrm{T}}.\end{aligned} \tag{12}$$

The next step, which is a modelisation step, is to close the expressions of the form $\mathscr{E}(\cdot)$. For example, in absence of mass transfer, it is of common use [7,21], to model

$$\mathscr{E}\left(P^{(k)} \nabla X^{(k)}\right) = P_{\mathrm{I}} \nabla \alpha^{(k)},$$

$$\mathscr{E}\left((P^{(k)}\mathbf{u}) \cdot \nabla X^{(k)}\right) = P_{\mathrm{I}}\mathbf{u}_{\mathrm{I}} \nabla \alpha^{(k)},$$

$$\mathscr{E}\left(\sigma \cdot \nabla X^{(k)}\right) = \mathbf{u}_{\mathrm{I}} \nabla \alpha^{(k)},$$

where P_{I} is an average interface pressure, $\mathbf{u}_{\mathrm{I}}$ is an average interface velocity. Relaxation terms were introduced [21] to modelise the terms omitted by this averaging procedure. Of course, the difficult question is how to define the interfacial quantities and the remaining terms, and there is a real debate about this. Another difficult question is, from a mathematical point of view, to define products like $P_{\mathrm{I}} \nabla \alpha^{(k)}$, where both P_{I} and $\alpha^{(k)}$ may be simultaneously discontinuous. In [21] we have developed a method that solves the second problem, at least for flows with no shock (only contacts) and no mass transfer between phases at shock fronts. This does not solve the problem in a general context since there may exist situations where a shock wave enter a zone where $\alpha^{(k)}$ is discontinuous.

In this paper, we try to follow a different path. We wish to model as few as possible, in particular, we want to avoid using interfacial average terms since their definition is very delicate, if possible. However, we want to follow the path developed in [7], which is summarised in Eqs. (1), (2), (4)–(8). The key point is to evaluate exactly the averages in (7) and (8). This can be done under mild assumptions that can be listed exhaustively. Our numerical method uses the same type of procedure *at the discrete level*.

2.2. Notations

Assuming two non-miscible phases Σ_1 and Σ_2 coexist in the flow, we consider the following notations throughout the paper:

- $U^{(k)}$, $k = 1, 2$ is the vector of conservative variables that describes the non-averaged flow,

$$U^{(k)} = (\rho^{(k)},\ \rho^{(k)}\mathbf{u}^{(k)},\ \rho^{(k)}E^{(k)})^{\mathrm{T}}.$$

  The notation $F^{(k)}$ is the associated flux,

$$F^{(k)} = (\rho^{(k)}\mathbf{u}^{(k)},\ \rho^{(k)}\mathbf{u}^{(k)} \otimes \mathbf{u}^{(k)} + P^{(k)}Id,\ (\rho^{(k)}E^{(k)} + P^{(k)})\mathbf{u}^{(k)})^{\mathrm{T}}.$$

  The vector $U = (U^{(1)}, U^{(2)})$ denotes

$$U = (\rho^{(1)},\ \rho^{(1)}\mathbf{u}^{(1)},\ \rho^{(1)}E^{(1)},\ \rho^{(2)},\ \rho^{(2)}\mathbf{u}^{(2)},\ \rho^{(2)}E^{(2)})^{\mathrm{T}}.$$

  $F = (F^{(1)}, F^{(2)})$ is the associated flux.
- $W^{(k)}$ is the vector of conserved averaged variables,

$$W^{(k)} = \alpha^{(k)}U^{(k)},$$

  and $\mathscr{F}^{(k)}$ is the corresponding flux. We also define $W = (W^{(1)}, W^{(2)})$ and $\mathscr{F} = (\mathscr{F}^{(1)}, \mathscr{F}^{(2)})$.
- $X^{(k)}$ is the characteristic function of the phase Σ_k, and by abuse of language, we also set $U^{(k)} = X^{(k)}U$, $W^{(k)} = X^{(k)}W$, etc.

More generally, if g is any flow variable, $g^{(k)}$ represents this flow variable for the phase Σ_k. When there is no ambiguity, without the superscript (k), the variable g denotes $g^{(1)}$.

3. Derivation of the numerical scheme

In this section, our purpose is to derive a semi-discrete numerical approximation of the two-phase system (1)–(7). For the sake of simplicity, we assume the flow consists in two non-miscible phases Σ_1 and Σ_2.

The scheme is of the finite volume type: the degrees of freedom are the averaged values of the conservative variables (9) on the control volumes $\{\mathscr{C}_i\}_i$, where $\cup_i \mathscr{C}_i = \Omega$, the computational domain. For the purpose of convenience, we denote $W^{(1)} = (\alpha^{(1)}\rho^{(1)},\ \alpha^{(1)}\rho^{(1)}u^{(1)},\ \alpha^{(1)}E^{(1)})^{\mathrm{T}}$ (resp. $W^{(2)} = (\alpha^{(2)}\rho^{(2)},\ \alpha^{(2)}\rho^{(2)}u^{(2)},\ \alpha^{(2)}E^{(2)})^{\mathrm{T}}$) the conserved variables for Σ_1 (resp. Σ_2) and $\mathscr{F}^{(1)}$ (resp. $\mathscr{F}^{(2)}$) the corresponding fluxes.

The idea is to apply the derivation presented in the previous section to this discrete situation. Thus we consider a set of realisation, then evaluate (with the notations of Section 2.1), for $k = 1, 2$,

$$\int_{\mathscr{C}_i} X^{(k)} \frac{\partial U^{(k)}}{\partial t}\,\mathrm{d}x + \int_{\mathscr{C}_i} X^{(k)} \frac{\partial F^{(k)}}{\partial x}\,\mathrm{d}x = 0$$

and make an ensemble average, i.e.,

$$\int_{\mathscr{C}_i} \frac{\partial W^{(k)}}{\partial t}\,\mathrm{d}x + \int_{\partial\mathscr{C}_i} \mathscr{F}^{(k)} \cdot \mathbf{n} = \int_{\mathscr{C}_j} \mathscr{E}\big(\mathscr{G}^{(k)}\big)\,\mathrm{d}x,$$

where, being consistent with (11), we have set

$$\mathscr{G}^{(k)} = ((\rho^{(k)}(\mathbf{u}^{(k)} - \sigma)) \cdot \nabla X^{(k)}, (\rho^{(k)}\mathbf{u}^{(k)} \otimes (\mathbf{u}^{(k)} - \sigma) + P^{(k)}) \cdot \nabla X^{(k)},\ (\rho^{(k)}E^{(k)}(\mathbf{u}^{(k)} - \sigma) + P^{(k)}\mathbf{u}^{(k)}) \cdot \nabla X^{(k)},\ \sigma \cdot \nabla X^{(k)}).$$

The evaluation of the various terms involved in the previous equations amount to solve the problem, for a general ensemble average! This is why we consider a simplified ensemble average which is constructed by considering bubbles that are collections of elementary bubbles with very simple shapes, see Fig. 3. We construct the repartition of bubbles in such a way that some of the moments of the repartition law are recovered. This is detailed in the next paragraph. The elementary bubbles have to be chosen in such a way that any bubble, in the limit, can be represented as an agglomeration of elementary bubbles, for example as in Fig. 3 where the elementary bubbles are rectangles.

Of course, even if this framework is considerably simplified with respect to real life, it is still too complex to perform effective calculations. This is why we precise the necessary assumptions needed to compute easily the various terms involved in the formula, i.e., to recover some moments of the repartion law. The derivation is first conducted in the one-dimensional case.

3.1. General principles and notations

We consider a computational mesh $(x_i)_{i\in\mathbb{Z}}$ and the associated control volumes $\mathscr{C}_i =]x_{i-1/2}, x_{i+1/2}[$ where as usual $x_{i+1/2} = (x_i + x_{i+1})/2$. On each control volume, the flow is approximated by the two vectors $W_i^{(1)} = (\alpha^{(1)}\rho_i^{(1)},\ \alpha_i^{(1)}\rho_i^{(1)}u_i^{(1)},\ \alpha_i^{(1)}E_i^{(1)})^{\mathrm{T}}$ and $W_i^{(2)} = (\alpha_i^{(2)}\rho_i^{(2)},\ \alpha_i^{(2)}\rho_i^{(2)}u_i^{(2)},\ \alpha_i^{(2)}E_i^{(2)})^{\mathrm{T}}$, where $\alpha_i^{(1)}$ and $\alpha_i^{(2)}$ are the volume fraction of the phases Σ_1 and Σ_2, $\alpha_i^{(1)} + \alpha_i^{(2)} = 1$.

The main idea of the method is to proceed in several steps:

1. consider at time t a random subdivision of each control volumes, $x_{i-1/2} = \xi_0 < \xi_1 < \cdots < \xi_{N(\omega)} = x_{i+1/2}$, where ω is a random parameter aimed at indexing that specific realisation and $N(\omega) - 2$ is the number of internal points (see Fig. 4);
2. affect randomly in each subcell $]\xi_l, \xi_{l+1}[$ the phases Σ_1 or Σ_2 with the state $U_i^{(1)} = (\rho_i^{(1)},\ \rho_i^{(1)}u_i^{(1)},\ E_i^{(1)})^{\mathrm{T}}$ and $U_i^{(2)} = (\rho_i^{(2)},\ \rho_i^{(2)}u_i^{(2)},\ E_i^{(2)})^{\mathrm{T}}$; this means in particular that $X^{(k)}$ is assumed constant in $]\xi_j, \xi_{j+1}[$, $0 \leqslant j \leqslant N(\omega) - 1$;
3. write the semi-discrete approximation of that realisation thanks to Godunov scheme;
4. make an ensemble average of all realisations.

We may assume that two adjacent *internal* interfaces contain different phases, because if not, we may merge the two internal cells. Hence, we merge similar adjacent internal cells; this has no consequences in the results because the scheme is of finite volume type. Of course, the most left internal cell of $\mathscr{C}_i$ and the most right internal cell of $\mathscr{C}_{i-1}$, whatever i, may contain the same phase, because the control volumes are considered independently.

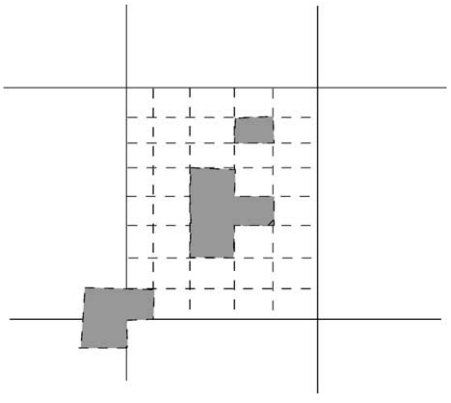

Fig. 3. A configuration for a simplified ensemble average where the bubbles are agglomerations of quadrangles.

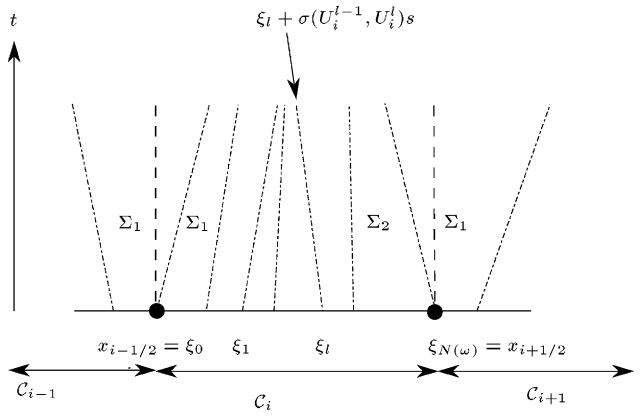

Fig. 4. A space–time configuration which shows a subdivision of the computational cell $\mathscr{C}_i$ as well as the deplacement of internal interfaces.

There is clearly a constraint on the subdivision and $N(\omega)$. We choose the subdivisions in such a way that the average length of all the internal sub-cells containing Σ_1 is $\alpha_i^{(1)}\Delta x$, that is

$$\mathscr{E}\left(\sum_{j=0}^{N(\omega)-1} X^{(k)}\left(\frac{\xi_j+\xi_{j+1}}{2}\right)(\xi_{j+1}-\xi_j)\right) = \Delta x \alpha_i^{(k)}. \tag{13}$$

Since the state U is constant in each $]\xi_j, \xi_{j+1}[$, we notice that

$$\mathscr{E}\left(\frac{1}{\Delta x}\int_{x_{i-1/2}}^{x_{i+1/2}} X^{(k)} U \,\mathrm{d}x\right) = W_i^{(k)};$$

so the control of the volume fraction plus the way we fill internal cells is enough to recover the average state, without any additional assumptions.

In the following, we use the following notations:

- $\mathscr{P}(A)$ the probability of an event A and $\mathscr{E}(G)$ the mathematical expectation of the random variable G,
- U_i^l is the conservative vector in the subcell $]\xi_l, \xi_{l+1}[$. We denote by U_i^+ the state in the most right subcell of $\mathscr{C}_i$ and U_i^- the state in the most left subcell of $\mathscr{C}_i$.

Doing so, the evolution of the phase Σ_1 in C_i obeys

$$\int_t^{t+s}\int_{C_i} X\left(\frac{\partial U}{\partial t}+\frac{\partial F}{\partial x}\right)\mathrm{d}x\,\mathrm{d}t = 0,$$

that is

$$\sum_{j=0}^{N(\omega)-1}\int_{\xi_j}^{\xi_{j+1}} X\frac{\partial U}{\partial t}\,\mathrm{d}x + \sum_{j=0}^{N(\omega)-1}\int_{\xi_j}^{\xi_{j+1}} X\frac{\partial F}{\partial x}\,\mathrm{d}x = 0, \tag{14}$$

where the characteristic function obeys

$$\sum_{j=0}^{N(\omega)-1}\int_t^{t+s}\int_{\xi_j}^{\xi_{j+1}} \frac{\partial X}{\partial t}\,\mathrm{d}x\,\mathrm{d}t + \sum_{j=0}^{N(\omega)-1}\int_t^{t+s}\int_{\xi_j}^{\xi_{j+1}} \sigma\frac{\partial X}{\partial x}\,\mathrm{d}x\,\mathrm{d}t = 0. \tag{15}$$

In this sum, there are two types of terms: the integral terms for $j = 1$ to $j = N(\omega) - 2$ which correspond to the internal subcells, and the terms $j = 1$ and $j = N(\omega) - 1$ which correspond to the boundary subcells. To evaluate easily these integrals, we observe that the interface between two subcells moves at the speed of the contact discontinuity between the left- and right-constant states U_{L} and U_{R} at that interface. We denote this speed by $\sigma(U_{\mathrm{L}}, U_{\mathrm{R}})$. This interface separates the two phases Σ_1 and Σ_2, so $U_{\mathrm{L}} = U^{(1)}$ and $U_{\mathrm{R}} = U^{(2)}$ or $U_{\mathrm{L}} = U^{(2)}$ and $U_{\mathrm{R}} = U^{(1)}$. For a given configuration, there is a finite number of internal subcells. Hence, between times t and $t + s$ with s small enough, the situation in $\mathscr{C}_i$ evolves like in Fig. 4: before the interfaces cross the cell boundary, each subcell is stretched or compressed according to the solutions of local Riemann problems, and the interfaces move at constant speeds.

We denote by $F(U_{\mathrm{L}}, U_{\mathrm{R}})$ the Godunov numerical flux between the states U_{L} and U_{R} and $F^{\mathrm{lag}}(U_{\mathrm{L}}, U_{\mathrm{R}})$ the flux across the contact discontinuity between the states U_{L} and U_{R}. Following the notations of Fig. 5, we have

$$F^{\mathrm{lag}}(U_{\mathrm{L}}, U_{\mathrm{R}}) = F(U^{+}_{\mathrm{LR}}) - \sigma(U_{\mathrm{L}}, U_{\mathrm{R}})U^{+}_{\mathrm{LR}} = F(U^{-}_{\mathrm{LR}}) - \sigma(U_{\mathrm{L}}, U_{\mathrm{R}})U^{-}_{\mathrm{LR}},$$

where superscripts $\pm$ denote the states on the right and the left of the contact discontinuity, respectively. We also denote by $U^{*}_{i+1/2}$ the solution of the Riemann problem between U^{+}_{i} and U^{-}_{i+1}.

The Riemann problems in each subcell are independent if the solution is sought for times $[t, t + s]$ for s that satisfies a CFL condition of the type

$$|\lambda_{\max}| \frac{s}{\Delta\xi} \leqslant \frac{1}{2}. \tag{16}$$

Here $\lambda_{\max}$ is the maximum wave speed and $\Delta\xi$ is the minimum width of a subcell. Then we integrate Eq. (14) between t and $t + s$, namely

$$\sum_{l=1}^{N(\omega)-1} \int_{t}^{t+s} \int_{\xi_l}^{\xi_{l+1}} X \frac{\partial U}{\partial t} \, \mathrm{d}x \, \mathrm{d}t + \sum_{t=1}^{N(\omega)-1} \int_{t}^{t+s} \int_{\xi_l}^{\xi_{l+1}} X \frac{\partial F}{\partial x} \, \mathrm{d}x \, \mathrm{d}t = 0 \tag{17}$$

and let $s \to 0$.

As in Fig. 6 let us call D' the point on the interface moving at speed $\sigma(U^{+}_{i-1}, U^{-}_{i})$ coming from $x_{i-1/2}$ and C' the analogous point for $x_{i+1/2}$. We denote by ADD' (resp. BCC') the space–time triangle that lies between the segment AD (resp. BC) and the characteristic AD' (resp. BC'). The space–time domain $\mathscr{C}_i \times [t, t + s]$ is

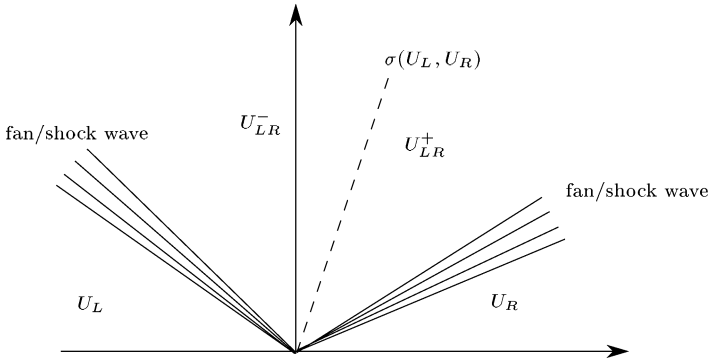

Fig. 5. The various states in the Riemann problem with the Euler equations between states U_{L} and U_{R}.

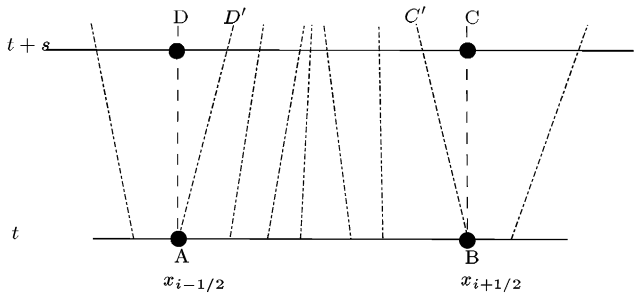

Fig. 6. Configuration for the evaluation of (17).

the reunion of $ADD' \cap \mathscr{C}_i$, $BCC' \cap \mathscr{C}_i$ and the Lagrangian internal cells as in Fig. 6. The triangle $ADD' \cap \mathscr{C}_i$ may be reduced to AD if $\sigma(U_{i-1}^+, U_i^-) \leqslant 0$. Similarly, area of $BCC' \cap \mathscr{C}_i$ may be reduced to CB if $\sigma(U_i^+, U_{i+1}^-) \geqslant 0$. These situations occur when the flow is going out of $\mathscr{C}_i$ from the left or the right. By abuse of language, in any case, we still denote $BCC' \cap \mathscr{C}_i$ (resp. $ADD' \cap \mathscr{C}_i$) by BCC' (resp. ADD').

Eq. (17) can be rewritten as

$$\begin{aligned}
&\int_{AD'D} X\left(\frac{\partial U}{\partial t}+\frac{\partial F}{\partial x}\right)\mathrm{d}x\,\mathrm{d}t && \text{(I)}\\
&+\sum_{l=2}^{N(\omega)-1}\int_{t_n}^{t+s}\int_{\xi_l+s\sigma(U_i^l,U_i^{l+1})}^{\xi_{l+1}+s\sigma(U_i^l,U_i^{l+1})} X\left(\frac{\partial U}{\partial t}+\frac{\partial F}{\partial x}\right)\mathrm{d}x\,\mathrm{d}t && \text{(II)}\\
&+\int_{CBB'} X\left(\frac{\partial U}{\partial t}+\frac{\partial F}{\partial x}\right)\mathrm{d}x\,\mathrm{d}t=0 && \text{(III)}.
\end{aligned} \tag{18}$$

We detail each term

Boundary terms (I) and (III): We consider first (I). We have

$$\begin{aligned}
\int_{AD'D} X\left(\frac{\partial U}{\partial t}+\frac{\partial F}{\partial x}\right)\mathrm{d}x\,\mathrm{d}t &= \int_{AD'D}\left(\frac{\partial XU}{\partial t}+\frac{\partial XF}{\partial x}\right)\mathrm{d}x\,\mathrm{d}t-\int_{AD'D}\left(U\frac{\partial X}{\partial t}+F(U)\frac{\partial X}{\partial x}\right)\mathrm{d}x\,\mathrm{d}t\\
&=\int_{x_{i-1/2}}^{x_{i-1/2}+s\sigma^+(U_{i-1}^+,U_i^-)} X(x,t+s)U(x,t+s)\,\mathrm{d}x - sX(x_{i-1/2},t^+)F(U_{i-1/2}^*)\\
&\quad + sF^{\mathrm{lag}}(U_{i-1}^+,U_i^0)[X]_{j=0}.
\end{aligned}$$

Here, we use the notation $a^+ = \max(0,a)$ and $[X]_l$ is the jump of X at node ξ_l. Similarly, we have for (III)

$$\begin{aligned}
\int_{BCC'} X\left(\frac{\partial U}{\partial t}+\frac{\partial F}{\partial x}\right)\mathrm{d}x\,\mathrm{d}s &= \int_{x_{i+1/2}}^{x_{i+1/2}+s\sigma^-(U_i^+,U_{i+1}^-)} X(x,t+s)U(x,t+s)\,\mathrm{d}x\,\mathrm{d}s - sX(x_{i-1/2},t^+)F(U_{i-1/2}^*)\\
&\quad + sF^{\mathrm{lag}}(U_i^+,U_{i+1}^-)[X]_{j=N(\omega)},
\end{aligned}$$

we have used the notation $a^- = \min(0,a)$. The "flowing away" cases are taken into account by the bound $x_{i-1/2}+s\sigma^+(U_{i-1}^+,U_i^-)$ in the case (I) and $x_{i+1/2}+s\sigma^-(U_i^+,U_{i+1}^-)$ in the case (III).

Internal terms (II): We have

$$\int_t^{t+s}\int_{\xi_j+s\sigma(U_i^{j-1},U_i^j)}^{\xi_{j+1}+s\sigma(U_i^j,U_i^{j+1})} X\left(\frac{\partial U}{\partial t}+\frac{\partial F}{\partial x}\right)\mathrm{d}x\,\mathrm{d}t = s\Big([X]_j F^{\mathrm{lag}}(U_i^j,U_i^{j+1})+[X]_{j-1}F^{\mathrm{lag}}(U_i^{j-1},U_i^j)\Big) + \int_{\xi_j+s\sigma(U_i^{j-1},U_i^j)}^{\xi_{j+1}+s\sigma(U_i^j,U_i^{j+1})} X(x,t+s)U(x,t+s)\,\mathrm{d}x - \int_{\xi_j}^{\xi_{j+1}} X(x,t)U(x,t)\,\mathrm{d}x.$$

If we sum up all the terms, we get

$$\begin{aligned}&\frac{1}{\Delta x}\int_{x_{i-1/2}}^{x_{i+1/2}} X(x,t+s)U(x,t+s)\,\mathrm{d}x - \frac{1}{\Delta x}\int_{x_{i-1/2}}^{x_{i+1/2}} X(x,t)U(x,t)\,\mathrm{d}x + \frac{s}{\Delta x}\Big(X(x_{i+1/2},t^+)F(U^*_{i+1/2})\\ &\quad - X(x_{i-1/2},t^+)F(U^*_{i-1/2})\Big)\\ &= \frac{1}{\Delta x}\sum_{j=1}^{N(\omega)-1} s\Big([X]_j F^{\mathrm{lag}}(U_i^j,U_i^{j-1})+[X]_{j-1}F^{\mathrm{lag}}(U_i^{j-1},U_i^{j-2})\Big) + s\Big(\frac{[X]_0}{\Delta x}F^{\mathrm{lag}}(U_{i-1}^+,U_i^-)\\ &\quad + \frac{[X]_{N(\omega)}}{\Delta x}F^{\mathrm{lag}}(U_i^+,U_{i+1}^-)\Big).\end{aligned}$$

Taking the limit when $s\to 0$, we have the semi-discrete scheme

$$\begin{aligned}&\frac{\mathrm{d}}{\mathrm{d}t}\left(\frac{1}{\Delta x}\int_{x_{i-1/2}}^{x_{i+1/2}} X(x,t)U(x,t)\,\mathrm{d}x\right) + \frac{1}{\Delta x}\Big(X(x_{i+1/2},t^+)F(U^*_{i+1/2}) - X(x_{i-1/2},t^+)F(U^*_{i-1/2})\Big)\\ &= \frac{1}{\Delta x}\sum_{j=1}^{N(\omega)-1}\Big([X]_j F^{\mathrm{lag}}(U_i^j,U_i^{j-1})+[X]_{j-1}F^{\mathrm{lag}}(U_i^{j-1},U_i^{j-2})\Big) + \frac{[X]_0}{\Delta x}F^{\mathrm{lag}}(U_{i-1}^+,U_i^-)\\ &\quad - \frac{[X]_{N(\omega)}}{\Delta x}F^{\mathrm{lag}}(U_i^+,U_{i+1}^-).\end{aligned} \tag{19}$$

Next, we take the mathematical expectancy of the relations (19). We first have

$$\mathscr{E}\left(\frac{1}{\Delta x}\int_{x_{i-1/2}}^{x_{i+1/2}} X(x,t)U(x,t)\right) = \alpha_i^{(1)}U_i^{(1)}.$$

Then, we consider

$$\sum_{j=1}^{N(\omega)-1}\Delta t\Big([X]_j F^{\mathrm{lag}}(U_i^l,U_i^{l-1})+[X]_{j-1}F^{\mathrm{lag}}(U_i^{j-1},U_i^{j-2})\Big).$$

We have $[X]_l = -[X]_{l-1} = 1$ thanks to the definition of ξ_l: through a sub-cell interface, X change from 0 to 1 or 1 to 0 depending whether we leave or not the considered phase. Hence,

$$\begin{aligned}&\sum_{j=1}^{N(\omega)-1}\Big([X]_j F^{\mathrm{lag}}(U_i^j,U_i^{j-1})+[X]_{j-1}F^{\mathrm{lag}}(U_i^{j-1},U_i^{j-2})\Big)\\ &= N(\omega)_{\mathrm{int}}\Big(F^{\mathrm{lag}}(U_i^{(2)},U_i^{(1)}) - F^{\mathrm{lag}}(U_i^{(1)},U_i^{(2)})\Big),\end{aligned} \tag{20}$$

where $N(\omega)_{\mathrm{int}}$ is the number of internal subcells.

This shows the expectancy of (19) is

$$\begin{aligned}&\frac{\mathrm{d}(\alpha_i^{(1)}U_i^{(1)})}{\mathrm{d}t}+\frac{1}{\Delta x}\left(\mathscr{E}\left(X(x_{i+1/2},t^+)F(U^*_{i+1/2})\right)-\mathscr{E}\left(X(x_{i-1/2},t^+)F(U^*_{i-1/2})\right)\right)\\&\quad=\frac{\mathscr{E}(N(\omega)_{\mathrm{int}})}{\Delta x}\left(F^{\mathrm{lag}}(U_i^{(2)},U_i^{(1)})-F^{\mathrm{lag}}(U_i^{(1)},U_i^{(2)})\right)+\frac{1}{\Delta x}\Big(\mathscr{E}([X]_0)F^{\mathrm{lag}}(U_{i-1}^+,U_i^-)\\&\qquad-\mathscr{E}([X]_{N(\omega)})F^{\mathrm{lag}}(U_i^+,U_{i+1}^-)\Big),\end{aligned}\tag{21}$$

where $\mathscr{E}(N(\omega)_{\mathrm{int}})/\Delta x$ is interpreted as the average number of internal interfaces.

It remains to evaluate the three terms $\mathscr{E}(X(x_{i+1/2},t^+)F(U^*_{i+1/2}))$, $\mathscr{E}(X(x_{i-1/2},t^+)F(U^*_{i-1/2}))$, and $\mathscr{E}([X]_0)F^{\mathrm{lag}}(U_{i-1}^+,U_i^-)-\mathscr{E}([X]_{N(\omega)})F^{\mathrm{lag}}(U_i^+,U_{i+1}^-)$. This is done in the next section.

3.2. Averaging procedure

Evaluation of conservative terms. We first consider cell boundary $i+1/2$ and focus on the fluxes available for fluid Σ_1, namely $\mathscr{E}(X(x_{i+1/2},t_n^+)F(U^*_{i+1/2}))$. On this cell boundary, four instances may occur: $U_{i+1}^-=U_{i+1}^{(1)}$ and $U_i^+=U_i^{(1)}$, $U_{i+1}^-=U_{i+1}^{(1)}$ and $U_i^+=U_i^{(2)}$, $U_{i+1}^-=U_{i+1}^{(2)}$ and $U_i^+=U_i^{(1)}$, $U_{i+1}^-=U_{i+1}^{(2)}$ and $U_i^+=U_i^{(2)}$. We define

$$\beta_{i+1/2}^{(l,p)}=\mathrm{sign}\,(\sigma(U_i^l,U_{i-1}^p))=\begin{cases}1 & \text{if } \sigma(U_i^l,U_{i-1}^p)\geqslant 0,\\ -1 & \text{if } \sigma(U_i^l,U_{i-1}^p)<0.\end{cases}$$

Last, we introduce $X(x^{\pm}_{i+1/2})=\lim_{x-x_{i+1/2}\to 0^{\pm}}X(x)$. With these notations, the four instances described above are summarised in Table 1.

Thus, we have

$$\begin{aligned}\mathscr{E}\left(X(x_{i+1/2},t_n^+)F(U^*_{i+1/2})\right)&=\mathscr{P}\left(X(x^-_{i+1/2})=1\text{ and }X(x^+_{i+1/2})=1\right)F(U_i^{(1)},U_{i+1}^{(1)})+\mathscr{P}\left(X(x^-_{i+1/2})\right.\\&\quad\left.=1\text{ and }X(x^+_{i+1/2})=0\right)\left(\beta_{i+1/2}^{(1,2)}\right)^+F(U_i^{(1)},U_{i+1}^{(2)})+\mathscr{P}\left(X(x^-_{i+1/2})\right.\\&\quad\left.=0\text{ and }X(x^+_{i+1/2})=1\right)\left(\beta_{i+1/2}^{(2,1)}\right)^+F(U_i^{(2)},U_{i+1}^{(1)}).\end{aligned}$$

It remains to evaluate the terms $\mathscr{P}_{i+1/2}(\Sigma_p,\Sigma_q)$ above

$$\begin{aligned}\mathscr{P}_{i+1/2}(\Sigma_1,\Sigma_1)&:=\mathscr{P}\left(X(x^-_{i+1/2})=1\text{ and }X(x^+_{i+1/2})=1\right),\\\mathscr{P}_{i+1/2}(\Sigma_1,\Sigma_2)&:=\mathscr{P}\left(X(x^-_{i+1/2})=1\text{ and }X(x^+_{i+1/2})=0\right),\\\mathscr{P}_{i+1/2}(\Sigma_2,\Sigma_1)&:=\mathscr{P}\left(X(x^-_{i+1/2})=0\text{ and }X(x^+_{i+1/2})=1\right),\\\mathscr{P}_{i+1/2}(\Sigma_2,\Sigma_2)&:=\mathscr{P}\left(X(x^-_{i+1/2})=0\text{ and }X(x^+_{i+1/2})=0\right).\end{aligned}\tag{22}$$

Table 1
The various flow configurations at cell boundary $i+1/2$

Flow patterns	Left and right states	Flux indicator
$\Sigma_1-\Sigma_2$	$U_i^{(1)},U_{i+1}^{(2)}$	$(\beta_{i+1/2}^{(1,2)})^+$
$\Sigma_1-\Sigma_1$	$U_i^{(1)},U_{i+1}^{(1)}$	1
$\Sigma_2-\Sigma_1$	$U_i^{(2)},U_{i+1}^{(1)}$	$(-\beta_{i+1/2}^{(2,1)})^+$
$\Sigma_2-\Sigma_2$	$U_i^{(2)},U_{i+1}^{(2)}$	0

This is carried out in Section 3.3.

Using these notations, we rewrite the terms arising at the interface $i+1/2$

$$\mathscr{E}\Big(X(x_{i+1/2},t_n^+)F(U^*_{i+1/2})\Big) = \mathscr{P}_{i+1/2}(\Sigma_1,\Sigma_2)\Big(\beta^{(1,2)}_{i+1/2}\Big)^+ F(U_i^{(1)},U_{i-1}^{(2)}) + \mathscr{P}_{i+1/2}(\Sigma_1,\Sigma_1)F(U_i^{(1)},U_{i-1}^{(1)}) + \mathscr{P}_{i+1/2}(\Sigma_2,\Sigma_1)\Big(-\beta^{(2,1)}_{i+1/2}\Big)^+ F(U_i^{(2)},U_{i+1}^{(1)}). \tag{23}$$

Let us consider now the cell boundary $(i-1/2)$. By the same arguments, we get the averaged flux $\mathscr{E}(X(x_{i-1/2},t_n^+)F(U^*_{i-1/2}))$ as follows:

$$\mathscr{E}\Big(X(x_{i-1/2},t_n^+)F(U^*_{i-1/2})\Big) = \mathscr{P}_{i-1/2}(\Sigma_1,\Sigma_2)\Big(\beta^{(1,2)}_{i-1/2}\Big)^+ F(U_{i-1}^{(1)},U_i^{(2)}) + \mathscr{P}_{i-1/2}(\Sigma_1,\Sigma_1)F(U_{i-1}^{(1)},U_i^{(1)}) + \mathscr{P}_{i-1/2}(\Sigma_2,\Sigma_1)\Big(-\beta^{(2,1)}_{i-1/2}\Big)^+ F(U_{i-1}^{(2)},U_i^{(1)}). \tag{24}$$

Evaluation of the non-conservative terms. We now consider the terms $\mathscr{E}([X]_0)F^{\mathrm{lag}}(U^+_{i-1},U^0_i)$ and $\mathscr{E}([X]_{N(\omega)})F^{\mathrm{lag}}(U_i^{N(\omega)},U^-_{i+1})$. We first consider the second term. As before, there are the same four possible configurations. The jump indicators are given in Table 2.

Using the same type of arguments as in the previous section, we have

$$\mathscr{E}([X]_{N(\omega)})F^{\mathrm{lag}}(U_i^{N(\omega)},U^-_{i+1}) = \mathscr{P}_{i+1/2}(\Sigma_1,\Sigma_2)\Big(\beta^{(1,2)}_{i+1/2}\Big)^- F^{\mathrm{lag}}(U_i^{(1)},U_{i+1}^{(2)}) - \mathscr{P}_{i+1/2}(\Sigma_2,\Sigma_1)\Big(\beta^{(2,1)}_{i+1/2}\Big)^- F^{\mathrm{lag}}(U_i^{(2)},U_{i+1}^{(1)}). \tag{25}$$

We now apply the same arguments to the most left interface. Again for this situation four instances may occur, and the same arguments give

$$\mathscr{E}([X]_0)F^{\mathrm{lag}}(U^+_{i-1},U^0_i) = -\mathscr{P}_{i-1/2}(\Sigma_1,\Sigma_2)\Big(\beta^{(1,2)}_{i-1/2}\Big)^+ F^{\mathrm{lag}}(U_{i-1}^{(1)},U_i^{(2)}) + \mathscr{P}_{i-1/2}(\Sigma_2,\Sigma_1)\Big(\beta^{(2,1)}_{i-1/2}\Big)^+ F^{\mathrm{lag}}(U_{i-1}^{(2)},U_i^{(1)}). \tag{26}$$

Relaxation terms. They are

$$\frac{\mathscr{E}(N_{\mathrm{int}})}{\Delta x}\Big(F^{\mathrm{lag}}(U_i^{(2)},U_i^{(1)}) - F^{\mathrm{lag}}(U_i^{(1)},U_i^{(2)})\Big), \tag{27}$$

where $\mathscr{E}(N_{\mathrm{int}})/\Delta x$ is the average number of internal interfaces per cell. These relaxation terms depend of the flow topology as we will see later on.

The volume fraction evolution scheme. The scheme is easily obtained from the previous calculations by setting $U=1$ and $F=0$. Doing this, $F^{\mathrm{lag}}(U_{\mathrm{L}},U_{\mathrm{R}})$ reduces to $-\sigma(U_{\mathrm{L}},U_{\mathrm{R}})$. Then the scheme reads

Table 2
The various ingredients for the computation of the non-conservative products related to the inner interface emerging from the cell boundary $i+1/2$

Flow pattern	Lagrangian flux	Jump indicator
$\Sigma_1-\Sigma_2$	$F^{\mathrm{lag}}(U_i^{(1)},U_{i+1}^{(2)})$	$\Big(\beta^{(1,2)}_{i+1/2}\Big)^-$
$\Sigma_1-\Sigma_1$	$F^{\mathrm{lag}}(U_i^{(1)},U_{i+1}^{(1)})$	0
$\Sigma_2-\Sigma_1$	$F^{\mathrm{lag}}(U_i^{(2)},U_{i+1}^{(1)})$	$-\Big(\beta^{(2,1)}_{i+1/2}\Big)^-$
$\Sigma_2-\Sigma_2$	$F^{\mathrm{lag}}(U_i^{(2)},U_{i+1}^{(2)})$	0

$$\frac{\mathrm{d}}{\mathrm{d}t}\alpha_i^{(1)} + \frac{1}{\Delta x}\Big[\mathscr{P}_{i-1/2}(\Sigma_1,\Sigma_2)\Big(\beta_{i-1/2}^{(1,2)}\Big)^{+}\sigma(U_{i-1}^{(1)},U_i^{(2)}) + \mathscr{P}_{i-1/2}(\Sigma_2,\Sigma_1)\Big(-\beta_{i-1/2}^{(2,1)}\Big)^{-}\sigma(U_{i-1}^{(2)},U_i^{(1)}) + \mathscr{P}_{i+1/2}(\Sigma_2,\Sigma_1)\Big(\beta_{i+1/2}^{(1,2)}\Big)^{+}\sigma(U_i^{(1)},U_{i+1}^{(2)}) + \mathscr{P}_{i+1/2}(\Sigma_2,\Sigma_1)\Big(-\beta_{i+1/2}^{(2,1)}\Big)^{-}\sigma(U_i^{(2)},U_{i+1}^{(1)})\Big] + \frac{\mathscr{E}(N_{\mathrm{int}})}{\Delta x}\Big(\sigma(U_i^{(2)},U_i^{(1)}) - \sigma(U_i^{(1)},U_i^{(2)})\Big) = 0. \tag{28}$$

3.3. Estimation of $\mathscr{P}_{i+1/2}(\Sigma_p,\Sigma_q)$

To estimate these terms, we make the following remarks. First,

$$\begin{aligned}\mathscr{P}_{i+1/2}(\Sigma_p,\Sigma_p) + \mathscr{P}_{i+1/2}(\Sigma_q,\Sigma_p) &= \alpha_{i+1}^p,\\ \mathscr{P}_{i+1/2}(\Sigma_p,\Sigma_p) + \mathscr{P}_{i+1/2}(\Sigma_p,\Sigma_q) &= \alpha_i^p\end{aligned} \tag{29}$$

whatever p and q, and

$$\mathscr{P}_{i+1/2}(\Sigma_p,\Sigma_q) \geqslant 0.$$

Since $0 \leqslant X(x_{i+1/2}^{\pm}) \leqslant 1$, we have

$$0 \leqslant X(x_{i+1/2}^{+})X(x_{i+1/2}^{-}) \leqslant X(x_{i+1/2}^{+})$$

and

$$0 \leqslant X(x_{i+1/2}^{+})X(x_{i+1/2}^{-}) \leqslant X(x_{i+1/2}^{-}),$$

so that $\mathscr{P}_{i+1/2}(\Sigma_p,\Sigma_p) \leqslant \alpha_i^p$ and $\mathscr{P}_{i+1/2}(\Sigma_p,\Sigma_p) \leqslant \alpha_{i+1}^p$. This means that

$$\mathscr{P}_{i+1/2}(\Sigma_p,\Sigma_p) \leqslant \min(\alpha_i^p,\alpha_{i+1}^p).$$

The second remark is that since

$$\mathscr{P}_{i+1/2}(\Sigma_p,\Sigma_p) \leqslant \min(\alpha_i^{(p)},\alpha_{i+1}^{(p)}),$$

we also have

$$\mathscr{P}_{i+1/2}(\Sigma_p,\Sigma_q) \geqslant \max(\alpha_i^{(p)} - \alpha_{i+1}^{(p)},0)$$

because

$$\mathscr{P}_{i+1/2}(\Sigma_q,\Sigma_p) = \alpha_{i+1}^p - \mathscr{P}_{i+1/2}(\Sigma_p,\Sigma_p) = \begin{cases}\alpha_{i+1}^p - \alpha_i^p \geqslant 0 & \text{if } \alpha_i^p \leqslant \alpha_{i+1}^p,\\ \alpha_{i+1}^p - \alpha_{i+1}^p) = 0 & \text{otherwise.}\end{cases}$$

We also notice that $\min(\alpha_i^p,\alpha_{i+1}^p) + \max(\alpha_i^p - \alpha_{i+1}^p,0) = 1$.

Moreover, if the flow is smooth, it is legitimate to ask that

$$\begin{aligned}\mathscr{P}_{i+1/2}(\Sigma_1,\Sigma_1) &= \mathscr{P}\Big(X(x_{i+1/2}^{+}) = 1 \text{ and } X(x_{i+1/2}^{-}) = 1\Big) \simeq \alpha^{(1)}(x_{i+1/2}),\\ \mathscr{P}_{i+1/2}(\Sigma_2,\Sigma_2) &= \mathscr{P}\Big(X(x_{i+1/2}^{+}) = 0 \text{ and } X(x_{i+1/2}^{-}) = 0\Big) \simeq \alpha^{(2)}(x_{i+1/2}),\\ \mathscr{P}_{i+1/2}(\Sigma_1,\Sigma_2) &= \mathscr{P}\Big(X(x_{i+1/2}^{+}) = 1 \text{ and } X(x_{i+1/2}^{-}) = 0\Big) \simeq 0,\\ \mathscr{P}_{i+1/2}(\Sigma_2,\Sigma_1) &= \mathscr{P}\Big(X(x_{i+1/2}^{+}) = 0 \text{ and } X(x_{i+1/2}^{-}) = 1\Big) \simeq 0.\end{aligned}$$

The first two relations are legitimate because they mean that, in the limit, the flow composition is approximately similar seen from the left and the right of $x_{i+1/2}$ almost everywhere. The last two means that almost nowhere, the flow composition may be different seen from the right and the left of $x_{i+1/2}$. Doing so, we implicitly assume that the flow is almost everywhere regular. This set of remarks is developed in Appendix A.

Combining all these remarks, we make the following estimation and assumption:

$$\mathscr{P}_{i+1/2}(\Sigma_p, \Sigma_p) = \min(\alpha_i^p, \alpha_{i+1}^p) \quad \text{whatever } p \text{ and } q. \tag{30}$$

From this, and using the relations (29), we get

$$\begin{aligned}
\mathscr{P}_{i+1/2}(\Sigma_1, \Sigma_1) &= \min\left(\alpha_i^{(1)}, \alpha_{i+1}^{(1)}\right),\\
\mathscr{P}_{i+1/2}(\Sigma_1, \Sigma_2) &= \max\left(\alpha_i^{(1)} - \alpha_{i+1}^{(1)}, 0\right),\\
\mathscr{P}_{i+1/2}(\Sigma_2, \Sigma_1) &= \max\left(\alpha_i^{(2)} - \alpha_{i+1}^{(2)}, 0\right),\\
\mathscr{P}_{i+1/2}(\Sigma_2, \Sigma_2) &= \min\left(\alpha_i^{(2)}, \alpha_{i+1}^{(2)}\right).
\end{aligned} \tag{31}$$

Relations (30) and (31) are only approximations. They axe justified by two additional remarks. First, in the two-dimensional situations of Fig. 7 the fluxes along the vertical interfaces can be computed by the same techniques as here, and the formulae are identical to the ones we have presented here, with the same coefficients $\mathscr{P}_{i+1/2}(\Sigma_p, \Sigma_q)$. The physical meaning of these coefficients, in the configuration of Fig. 7, is the geometrical length of the common interface between two equivalent bubbles.

The second justification is more mathematical. Because our scheme is an *averaged* classical finite volume scheme, we may follow the lines of the proof of the Lax–Wendroff theorem, see e.g. [11]. We define W_Δ by

$$W_\Delta(x,t) = W_i^n \quad \text{if } (x,t) \in]x_{i-1/2}, x_{i+1/2}[\times[t_n, t_{n+1}[.$$

Thus, if we assume that, for $\Delta t/\Delta x$ fixed,

- the sequence W_Δ is bounded in $L^\infty(\mathbb{R}^+ \times \mathbb{R})$,
- there exists $W \in L^2(\mathbb{R} \times \mathbb{R}^+)_{\text{loc}}$ such that $W_\Delta \to W$,
- the probability law of the flow is known,
- $\mathscr{P}_{i+1/2}(\Sigma_p, \Sigma_q)$ has the functional form $\mathscr{P}_{i+1/2}(\Sigma_p, \Sigma_q) = P_{pq}(\alpha_i^{(p)}, \alpha_{i+1}^{(q)})$ with $(\alpha, \alpha') \mapsto P_{pq}(\alpha, \alpha')$ continuous and $P_{pp}(\alpha, \alpha) = \alpha$, $P_{pq}(\alpha, \alpha) = 0$ if $p \neq q$,

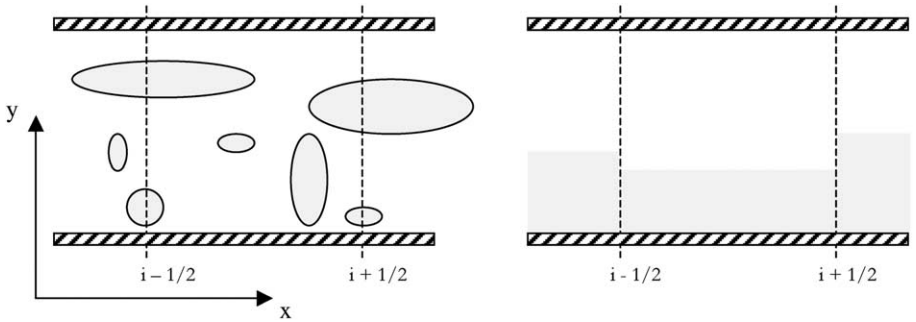

Fig. 7. Schematic representation of the equivalence between a bubbly flow or a dropplet flow with a stratified flow for the computation the numerical fluxes between at a cell boundary.

then the limit solution W satisfies, for any test function φ compactly supported on $\mathbb{R}\times\mathbb{R}^+$,

$$\int_{\mathbb{R}\times\mathbb{R}^+} W\frac{\partial\varphi}{\partial t}+F(W)\nabla\varphi-\int_{\mathbb{R}}W(x,0)\varphi(x,0)=\mathscr{E}\left(\int_{\mathbb{R}\times\mathbb{R}^+}(F(W)-\sigma W)\nabla X\varphi\right).$$

In other terms, the solution is a weak solution of the problem, as defined in [7]. This result is proved in Appendix A.

In practice, it is not necessary to know the probability law defined for the flow under study. We only compute averages, so it is only necessary to define averages. Here, the parameter that is given is the relaxation parameter, in other words, the expectancy of the number of internal bubbles.

The definition of $\mathscr{P}_{i+1/2}(\Sigma_p,\Sigma_q)$ above satisfies these assumptions. We have set this result for the Godunov scheme. In fact, what is really essential is that the numerical flux be continuous and that it is possible to have a discrete interface velocity.

3.4. Summary and extension to other fluxes

We end this section by a summary of the results. The numerical approximation of (7), for Σ_1, is

$$\frac{\mathrm{d}}{\mathrm{d}t}\left(\alpha_i^{(1)}U_i^{(1)}\right)+\frac{\mathscr{E}(XF)_{i+1/2}-\mathscr{E}(XF)_{i-1/2}}{\Delta x}=\mathscr{E}\left(F^{\mathrm{lag}}\frac{\partial X}{\partial x}\right),\tag{32}$$

where the various terms are defined below.

In (32), the numerical flux F that we use at the microscopic level is obtained thanks to an approximate Riemann solver for which it is possible to define a contact speed. The contact speed between the left state U_{L} and the right state U_{R} is denoted by $\sigma(U_{\mathrm{L}},U_{\mathrm{R}})$. We also denote by $U^{\pm}_{\mathrm{LR}}$ the left and right states surrounding the approximate contact discontinuity, similarly as in Fig. 5 for the Godunov solver. This permits to define the Lagrangian flux $F^{\mathrm{lag}}(U_{\mathrm{L}},U_{\mathrm{R}})=F(U^+_{\mathrm{LR}})-\sigma(U_{\mathrm{L}},U_{\mathrm{R}})U^+_{\mathrm{LR}}=F(U^-_{\mathrm{LR}})-\sigma(U_{\mathrm{L}},U_{\mathrm{R}})U^-_{\mathrm{LR}}$. Last, we define $\beta^{(p,q)}_{i+1/2}=\mathrm{sign}\,(\sigma(U_i^{(p)},U_{i+1}^{(q)}))$.

All the calculations have been performed for the Godunov scheme, but can be extended to more general fluxes. The key ingredient of the derivation are, besides the randomisation, average procedures and estimation of the various coefficients, the use of a Riemann solver for which it is possible to define a contact discontinuity speed. This property is needed because we must define a Lagrangian flux, $F^{\mathrm{lag}}(U,V)$, This Lagrangian flux has to be consistent, as well as the base flux $F(U,V)$,

Even more, the choice of the base flux F and the lagrangian flux F^{lag} may be independent: we do not really need a relation of the type $F^{\mathrm{lag}}=F^*-\sigma U^*$. This can easily be understood from the proof of the Lax–Wendroff theorem, see Appendix A.

The choice of the various fluxes has to be done only with the constraints of physical problem under study, there is a lot of freedom. In this paper, we have used the Godunov scheme and the HLLC flux [25].

Then, we have

$$\begin{aligned}\mathscr{E}(XF)_{i+1/2}&=\max(\alpha_i^{(1)}-\alpha_{i+1}^{(1)},0)\left(\beta^{(1,2)}_{i+1/2}\right)^+F(U_i^{(1)},U_{i+1}^{(2)})+\min(\alpha_i^{(1)},\alpha_{i+1}^{(1)})F(U_i^{(1)},U_{i+1}^{(1)})\\&\quad+\max(\alpha_i^{(2)}-\alpha_{i+1}^{(2)},0)\left(-\beta^{(2,1)}_{i+1/2}\right)^-F(U_i^{(2)},U_{i+1}^{(1)})\end{aligned}\tag{33}$$

and

$$\begin{aligned}\mathscr{E}\left(F^{\mathrm{lag}}\frac{\partial X}{\partial x}\right)_i &= \max(\alpha_i^{(1)}-\alpha_{i+1}^{(1)},0)\left(\beta_{i+1/2}^{(1,2)}\right)^{-}F^{\mathrm{lag}}(U_i^{(1)},U_{i+1}^{(2)})\\ &\quad-\max(\alpha_i^{(2)}-\alpha_{i+1}^{(2)},0)\left(\beta_{i+1/2}^{(2,1)}\right)^{-}F^{\mathrm{lag}}(U_i^{(2)},U_{i+1}^{(1)})\\ &\quad-\max(\alpha_{i-1}^{(1)}-\alpha_i^{(1)},0)\left(\beta_{i-1/2}^{(1,2)}\right)^{+}F^{\mathrm{lag}}(U_{i-1}^{(1)},U_i^{(2)})\\ &\quad+\max(\alpha_{i-1}^{(2)}-\alpha_i^{(2)},0)\left(\beta_{i-1/2}^{(2,1)}\right)^{+}F^{\mathrm{lag}}(U_{i-1}^{(2)},U_i^{(1)})+\Lambda_i\left(F^{\mathrm{lag}}(U_i^{(2)},U_i^{(1)})-F(U_i^{(1)},U_i^{(2)})\right),\end{aligned} \tag{34}$$

where

$$\Lambda_i=\frac{\mathscr{E}(N_{\mathrm{int}})}{\Delta x} \tag{35}$$

is the average number of internal interfaces. Similar expressions hold for the fluid Σ_2.

Last, the volume fraction evolution equation is obtained by the same formulas by setting $U=1$ and $F=0$ as done in Eq. (28). This means that the volume fraction equation comes from a trivial PDE

$$\frac{\partial 1}{\partial t}+\nabla.(0)=0. \tag{36}$$

3.5. Numerical approximation of the semi-discrete scheme

In Eq. (32), the term $\mathscr{E}(F^{\mathrm{lag}}(\partial X/\partial x))_i$ can be split into two parts

$$\mathscr{E}\left(F^{\mathrm{lag}}\frac{\partial X}{\partial x}\right)_i=\mathscr{E}\left(F^{\mathrm{lag}}\frac{\partial X}{\partial x}\right)_{i,\mathrm{bound}}+\mathscr{E}\left(F^{\mathrm{lag}}\frac{\partial X}{\partial x}\right)_{i,\mathrm{relax}},$$

where

$$\mathscr{E}\left(F^{\mathrm{lag}}\frac{\partial X}{\partial x}\right)_{i,\mathrm{relax}}=\Lambda_i\left(F^{\mathrm{lag}}(U_i^{(2)},U_i^{(1)})-F^{\mathrm{lag}}(U_i^{(1)},U_i^{(2)})\right)$$

and $\mathscr{E}(F^{\mathrm{lag}}(\partial X/\partial x))_{i,\mathrm{bound}}$ is defined by Eqs. (25) and (26).

In practical applications, the solution is reached via a splitting method. First, we integrate

$$\frac{\left(\alpha_i^{(1)}U_i^{(1)}\right)^{n+1/2}-\left(\alpha_i^{(1)}U_i^{(1)}\right)^{n}}{\Delta t}+\frac{\mathscr{E}(XF)_{i+1/2}-\mathscr{E}(XF)_{i-1/2}}{\Delta x}=\mathscr{E}\left(F^{\mathrm{lag}}\frac{\partial X}{\partial x}\right)_{i,\mathrm{bound}}. \tag{37}$$

This step is stable under the condition

$$|\lambda_{\max}|\frac{\Delta t}{\Delta x}\leqslant\frac{1}{2}. \tag{38}$$

Here $\lambda_{\max}$ is the maximum wave speed and Δx is the cell size. This condition holds because all internal waves are omitted during this evolution step.

Then, a relaxation step is applied

$$\frac{\left(\alpha_i^{(1)}U_i^{(1)}\right)^{n+1}-\left(\alpha_i^{(1)}U_i^{(1)}\right)^{n+1/2}}{\Delta t}=\mathscr{E}\left(F^{\mathrm{lag}}\frac{\partial X}{\partial x}\right)_{i,\mathrm{relax}}. \tag{39}$$

The fluxes are computed at time t_n. The relaxation step can be carried out by several ways

- by a standard resolution of (39) when Λ_i is not too large,
- by a procedure that computes the steady state of (39) when Λ_i is large. Such a relaxation procedure is detailed in [21,24].

When dealing with contact-interface problems at the macroscopic scale, as well as with well-mixed materials (for example solid alloys), the relaxation procedures given in [24] are appropriate. When dealing with mixtures containing a moderate number of interfaces per computational cell, the resolution of (39) is recommended. It is also possible in such situations to solve a micro-mechanical problem with integro-differential equations as was done in [10,16] or to use empirical closure laws including dissipation effects, as done in most two-phase flow codes.

4. Second-order accuracy

In this section, we propose an extension of the conventional MUSCL approach to get a second-order approximation of the scheme

$$\frac{\left(\alpha_i^{(1)}U_i^{(1)}\right)^{n+1}-\left(\alpha_i^{(1)}U_i^{(1)}\right)^{n}}{\Delta t}+\frac{\mathscr{E}(XF)_{i+1/2}-\mathscr{E}(XF)_{i-1/2}}{\Delta x}=\mathscr{E}\left(F^{\mathrm{lag}}\frac{\partial X}{\partial x}\right)_i, \tag{40}$$

where the fluxes are given by (33) and the non-conservative terms/relaxation by (34).

Following the MUSCL strategy, the variables U, defined by (9), in the systems (7) and (8) are approximated by their averaged values over the control volume $\{]x_{i-1/2},x_{i+1/2}[\}_{i\in\mathbb{Z}}$, so second-order accuracy can be achieved if we have a second-order accurate approximation of the average of $\partial F/\partial x$ (where F is the flux (10)) and $\mathscr{E}(\mathscr{G})$ (from (12)).

4.1. A predictor–corrector scheme

This scheme is an extension of the predictor–corrector scheme for a general conservation law $\partial W/\partial t+\partial G/\partial x=0$ that we recall. Here, the mesh size is Δy which is assumed uniform for simplicity only.

Step 1. From $\{W_j^n\}$, compute the (limited) slopes δW_i^n and evaluate

$$W_{i-1/2,r}^n=W_i^n-\frac{\Delta y}{2}\delta W_i^n,$$
$$W_{i+1/2,l}^n=W_i^n-\frac{\Delta y}{2}\delta W_i^n.$$

Step 2. Evolve the solution over half a time step

$$W_i^{n+1/2}=W_i^n-\frac{\Delta t}{2\Delta y}\left(G(W_{i+1/2,l}^n,+W_{i+1/2,r}^n)-G(W_{i-1/2,l}^n,W_{i-1/2,r}^n)\right).$$

Step 3. From $\{W_j^{n+1/2}\}$, evaluate the (limited) slopes $\delta W_j^{n+1/2}$, and compute

$$W_{i-1/2,r}^{n+1/2}=W_i^{n+1/2}-\frac{\Delta y}{2}\delta W_i^{n+1/2},$$
$$W_{i+1/2,l}^{n+1/2}=W_i^{n+1/2}+\frac{\Delta y}{2}\delta W_i^{n+1/2}.$$

Step 4. Compute

$$W_i^{n+1} = W_i^n - \frac{\Delta t}{\Delta y}\Big(G(W_{i+1/2,l}^{n+1/2}, W_{i+1/2,r}^{n+1/2}) - G(W_{i-1/2,l}^{n+1/2}, W_{i-1/2,r}^{n+1/2})\Big).$$

This is not the simplest predictor–corrector algorithm, see [25] for example, but the steps 1 and 2 are identical to the steps 3 and 4. Hence, it is very simple from the algorithmic point of view. Thanks to this remark, we only describe the corrector step of our second-order algorithm, i.e., the extension of steps 3 and 4.

4.2. A predictor–corrector scheme for multiphase flows

We start by the data reconstruction. Since the volume fraction has to remain between 0 and 1, and because of the constraint $\rho_k \geqslant 0$ and $P_k \geqslant 0$, we choose to reconstruct linearly the vector of primitive variables V_i^n where $V = (\alpha,\ \rho,\ u,\ P)^{\mathrm{T}}$ for each fluid. We extrapolate these variables by using their limited slopes $\delta_i V$:

$$V_i^n(x) = V_i^n + \frac{x - x_i}{2}\delta_i V$$

with $x \in]x_{i-1/2}, x_{i+1/2}[$. We denote by

$$V_{i-1/2,r}^n = V_i^n - \frac{\Delta x}{2}\delta_i V \quad \text{and} \quad V_{i+1/2,l}^n = V_i^n + \frac{\Delta x}{2}\delta_i V$$

the primitive variables at the most left/right points of the cell $]x_{i-1/2}, x_{i+1/2}[$. We denote by $U_{i\pm1/2,r}^n$ (resp. $U_{i\pm1/2,l}^n$) the vector of conservative variables corresponding to $V_{i\pm1/2,r}^n$ (resp. $V_{i\pm1/2,l}^n$).

In order to get an approximation of (7) and (8), we divide the cell $]x_{i-1/2}, x_{i+1/2}[$ into subintervals $]x_{i-1/2}, y_1[,]y_l, y_{l+1}[, l = 1, N-1,]y_N, x_{i+1/2}[$. In the cells $]y_l, y_{l+1}[$, we consider the conservative variable $W_{l+1/2}$ corresponding to the primitive variables $V_i^n(y_{l+1/2})$ with $y_{l+1/2} = (y_l + y_{l+1})/2$, in $]x_{i-1/2}, y_1[$ we consider the one corresponding to $V_{i-1/2,l}^n = V_i^n - \frac{1}{2}\delta_i V$, and similarly in $]\xi_N, x_{i+1/2}[$, we consider $V_{i+1/2,r}^n$. Then we apply the scheme (40), that is the technique developed in Section 3, to this data distribution. This means that we subdivide each interval into random sub-interval (with the constraints of Section 3), and then we take the expectancy of the schemes. There is no contradiction, since there might be only one random subdivision in each $]y_l, y_{l+1}[$: this is taken into account in the relaxation term of Eq. (35), which is defined here for *each* subinterval $]y_l, y_{l+1}[$, and might vary with respect to l. To indicate this variation, we denote it by $\Lambda(y_{l+1/2})$. Then, we get the averaged flux variation over the interval $]x_{i-1/2}, x_{i+1/2}[$ but summing up the contribution over each subinterval $x_{i-1/2}, y_1[,]y_l, y_{l+1}[$ for $l = 1, \ldots, N-1$ and $]y_N, x_{i+1/2}[$. The arguments in the formula (31) are those defined by the reconstructed left and right states at $x_{i\pm1/2}$. Similarly, $\beta_{i\pm1/2}^{(1,2)}$ represents the sign of the contact speed evaluated at $x_{i\pm1/2}$ from the reconstructed data.

In Step 3, the conservative terms sum up to

$$\begin{aligned}
\mathscr{E}(XF)_{i-1/2}^{(1)} &= (\beta_{i-1/2}^{(1,2)})^{+}\mathscr{P}_{i-1/2}(\Sigma_1,\Sigma_2)F(U_{i-1/2,l}^{(1),n+1/2}, U_{i-1/2,r}^{(2),n+1/2}) + \mathscr{P}_{i-1/2}(\Sigma_1,\Sigma_1)F(U_{i-1/2,l}^{(1),n+1/2}, U_{i-1/2,r}^{(1),n+1/2}) \\
&\quad - (\beta^{(2,1)})^{-}\mathscr{P}_{i-1/2}(\Sigma_2,\Sigma_1)F(U_{i-1/2,l}^{(2),n+1/2}, U_{i-1/2,r}^{(1),n+1/2}), \\
\mathscr{E}(XF)_{i+1/2}^{(1)} &= (\beta^{(1,2)})^{+} + \mathscr{P}_{i+1/2}(\Sigma_1,\Sigma_2)F(U_{i+1/2,l}^{(1),n+1/2}, U_{i+1/2,r}^{(2),n+1/2}) + \mathscr{P}_{i+1/2}(\Sigma_1,\Sigma_1)F(U_{i+1/2,l}^{(1),n+1/2}, U_{i+1/2,r}^{(1),n+1/2}) \\
&\quad - (\beta^{(2,1)})^{-}\mathscr{P}_{i+1/2}(\Sigma_2,\Sigma_1)F(U_{i+1/2,l}^{(2),n+1/2}, U_{i+1/2,r}^{(1),n+1/2})
\end{aligned} \tag{41}$$

since all the internal contributions cancel. The non-conservative terms

$$\mathscr{E}\left(F^{\mathrm{lag}}\frac{\partial X}{\partial x}\right)_i, = \mathscr{E}\left(F^{\mathrm{lag}}\frac{\partial X}{\partial x}\right)_{i,\mathrm{bound}} + \mathscr{E}\left(F^{\mathrm{lag}}\frac{\partial X}{\partial x}\right)_{i,\mathrm{relax}}$$

sum up to

$$
\begin{aligned}
&-(\beta^{(1,2)})^{+}\mathscr{P}_{i+1/2}(\Sigma_1,\Sigma_2)F^{\mathrm{lag}}(U^{(1),n}_{i-1/2,l},U^{(2),n}_{i-1/2,r})+(\beta^{(2,1)})^{+}\mathscr{P}_{i+1/2}(\Sigma_2,\Sigma_1)F^{\mathrm{lag}}(U^{(2),n}_{i-1/2,l},U^{(1),n}_{i-1/2,r})\\
&-(\beta^{(1,2)})^{-}\mathscr{P}_{i+1/2}(\Sigma_1,\Sigma_2)F^{\mathrm{lag}}(U^{(1),n}_{i-1/2,l},U^{(2),n}_{i-1/2,r})+(\beta^{(2,1)})^{-}\mathscr{P}_{i+1/2}(\Sigma_2,\Sigma_1)F^{\mathrm{lag}}(U^{(2),n}_{i-1/2,l},U^{(1),n}_{i-1/2,r})\\
&+\sum_{l=1}^{N-1}\max\left(0,\Delta\alpha^{(1)}(y_{l+1/2})\right)F^{\mathrm{lag}}(U_2^{(2),n}(y_{l+1/2}),U_1^{(1),n}(y_{l+1/2}))\\
&-\sum_{l=1}^{N-1}\max\left(0,\Delta\alpha^{(2)}(y_{l+1/2})\right)F^{\mathrm{lag}}(U_2^{(2),n}(y_{l+1/2}),U_1^{(1),n}(y_{l+1/2}))\\
&+\sum_{l=1}^{N-1}\Lambda(y_{l+1/2})\Big(F^{\mathrm{lag}}(U_2^{(2),n}(y_{l+1/2}),U_1^{(1),n}(y_{l+1/2}))-F^{\mathrm{lag}}(U_1^{(1),n}(y_{l+1/2}),U_2^{(2),n}(y_{l+1/2}))\Big),
\end{aligned}
\tag{42}
$$

where

$$\Delta\alpha^{(1)}(y_{l+1/2})=(\delta_i\alpha^{(1)})(\xi_l-\xi_{l+1}).$$

We do not need any β terms because we account for all the internal cells in $]x_{i-1/2},x_{i+1/2}[$. Hence, the last two terms of (42) are equal to

$$
\begin{aligned}
&\left(\sum_{l=1}^{N-1}F^{\mathrm{lag}}(U^{(2),n}(y_{l+1/2}),U^{(1),n}(y_{l+1/2}))(y_l-y_{l+1})\right)\max\left(0,\delta_i\alpha^{(1)}\right)\\
&-\left(\sum_{l=1}^{N-1}F^{\mathrm{lag}}(U^{(1),n}(y_{l+1/2}),U^{(2),n}(y_{l+1/2}))(y_l-y_{l+1})\right)\max\left(0,\delta_i\alpha^{(2)}\right)
\end{aligned}
$$

which converges, when $N\to\infty$ to

$$
\begin{aligned}
&\left(\int_{x_{i-1/2}}^{x_{i+1/2}}F^{\mathrm{lag}}(U^{(2),n}(y),U^{(1),n}(y))\,\mathrm{d}y\right)\max\left(0,\delta_i\alpha^{(1)}\right)\\
&-\left(\int_{x_{i-1/2}}^{x_{i+1/2}}F^{\mathrm{lag}}(U^{(1),n}(y),U^{(2),n}(y))\,\mathrm{d}y\right)\max\left(0,\delta_i\alpha^{(2)}\right).
\end{aligned}
\tag{43}
$$

Then we apply the mid-point rule to (43), and we have a second-order approximation of the non-conservative terms by

$$
\begin{aligned}
\Delta x\mathscr{E}\left(F^{\mathrm{lag}}\frac{\partial X}{\partial x}\right)=&-(\beta^{(1,2)})^{+}\mathscr{P}_{i+1/2}(\Sigma_1,\Sigma_2)F^{\mathrm{lag}}(U^{(1),n}_{i-1/2,l},U^{(2),n}_{i-1/2,r})\\
&+(\beta^{(2,1)})^{+}\mathscr{P}_{i+1/2}(\Sigma_2,\Sigma_1)F^{\mathrm{lag}}(U^{(2),n}_{i-1/2,l},U^{(1),n}_{i-1/2,r})\\
&-(\beta^{(1,2)})^{-}\mathscr{P}_{i+1/2}(\Sigma_1,\Sigma_2)F^{\mathrm{lag}}(U^{(1),n}_{i-1/2,l},U^{(2),n}_{i-1/2,r})\\
&+(\beta^{(2,1)})^{-}\mathscr{P}_{i+1/2}(\Sigma_2,\Sigma_1)F^{\mathrm{lag}}(U^{(2),n}_{i-1/2,l},U^{(1),n}_{i-1/2,r})\\
&+\max\left(0,\Delta\alpha_i^{(1)}\right)F^{\mathrm{lag}}(U_i^{(2),n},U_i^{(1),n})-\max\left(0,\Delta\alpha_i^{(2)}\right)F^{\mathrm{lag}}(U_i^{(1),n},U_i^{(2),n}),
\end{aligned}
\tag{44}
$$

where $\Delta\alpha_i^{(1)}=\alpha^{(1)}_{i+1/2,l}-\alpha^{(1)}_{i-1/2,r}$ and $\Delta\alpha_i^{(2)}=\alpha^{(2)}_{i+1/2,l}-\alpha^{(2)}_{i-1/2,r}$ are the limited slope of $\alpha^{(1)}$ and $\alpha^{(2)}$ in the cell C_i.

Similarly, the relaxation terms corresponding to a linear reconstruction of the data can be approximated, thanks to the same interpretation in terms of Riemann sums and to the mid-point rule by

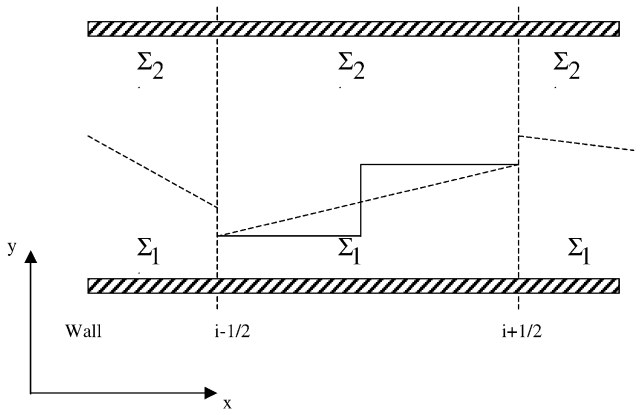

Fig. 8. Schematic representation of a computational cell with a gradient of volume fraction. The gradient in dotted lines is equivalent to the discontinuous representation with full lines.

$$\Lambda_i\Big(F^{\mathrm{lag}}(U_i^{(2),n},U_i^{(1),n})-F(U_i^{(1),n},U_i^{(2),n})\Big). \tag{45}$$

It is not surprising to have the averaged values of the conservative variables U_1 and U_2 because we need to evaluate $U^{(1)}$ and $U^{(2)}$ at the point $x_{i+1/2}$. This values are precisely the averaged ones thanks to the geometry of the cell. The same remark applies to the relaxation term Λ_i.

In the end, the predictor step becomes

$$\frac{(\alpha_i^{(1)}U_i^{(1)})^{n+k}-(\alpha_i^{(1)}U_i^{(1)})^{n}}{\Delta t}+\frac{\mathscr{E}(XF)_{i+1/2}^{(1)}-\mathscr{E}(XF)_{i-1/2}^{(1)}}{\Delta x}=\mathscr{E}\left(F^{\mathrm{lag}}\frac{\partial X}{\partial x}\right)_i, \tag{46}$$

where $\mathscr{E}(F^{\mathrm{lag}}(\partial X/\partial x))_i$ is the sum of (45) and (43), the conservative terms $\mathscr{E}(XF)_{i\pm1/2}^{(1)}$ are given by (41).

There is an enlightening interpretation of the scheme. It is important to note that the cell contains now a gradient of volume fraction α. Geometrically speaking, the mid-point rule applied to the integral of F^{lag} and the internal relaxation terms is equivalent to adding a new internal interface in the middle of the cell between the values $V_{i-1/2,l}^{(n)}$ and $V_{i+1/2,r}^{(n)}$ as depicted in Fig. 8.

It is essential to take into account this new interface for the design of the second-order scheme.

5. Some useful verifications

The various numerical approximations being rather complex, it is necessary to check some elementary properties. The following verifications may be done with the first- and the second-order variants. For the sake of conciseness we consider the first-order method only.

5.1. Uniform pressure and velocity flows

We have shown in a series of papers [2,21,22] that these uniform conditions were particularly important for interface problems. We consider the semi discrete form

$$\frac{\mathrm{d}}{\mathrm{d}t}\left(\alpha_i^{(1)}U_i^{(1)}\right)+\frac{\mathscr{E}(XF)_{i+1/2}^{(2)}-\mathscr{E}(XF)_{i-1/2}^{(2)}}{\Delta x}=\mathscr{E}\left(F^{\mathrm{lag}}\frac{\partial X}{\partial x}\right)_{i,\mathrm{bound}}, \tag{47}$$

where, for any i,

$$\mathscr{E}(XF)_{i+1/2} = \max\left(\alpha_i^{(1)} - \alpha_{i+1}^{(1)}, 0\right)\left(\beta_{i+1/2}^{(1,2)}\right)^{+} F(U_i^{(1)}, U_{i+1}^{(2)}) + \min\left(\alpha_i^{(1)}, \alpha_{i+1}^{(1)}\right) F(U_i^{(1)}, U_{i+1}^{(1)}) - \max\left(\alpha_i^{(2)} - \alpha_{i+1}^{(2)}, 0\right)\left(\beta_{i+1/2}^{(2,1)}\right)^{-} F(U_i^{(2)}, U_{i+1}^{(1)}) \tag{48}$$

and

$$\begin{aligned}\mathscr{E}\left(F^{\mathrm{lag}}\frac{\partial X}{\partial x}\right)_{i,\mathrm{bound}} = {} & \max\left(\alpha_i^{(1)} - \alpha_{i+1}^{(1)}, 0\right)\left(\beta_{i+1/2}^{(1,2)}\right)^{-} F^{\mathrm{lag}}(U_i^{(1)}, U_{i+1}^{(2)}) \\ & - \max\left(\alpha_i^{(2)} - \alpha_{i+1}^{(2)}, 0\right)\left(\beta_{i+1/2}^{(2,1)}\right)^{-} F^{\mathrm{lag}}(U_i^{(2)}, U_{i+1}^{(1)}) \\ & - \max\left(\alpha_{i-1}^{(1)} - \alpha_i^{(1)}, 0\right)\left(\beta_{i-1/2}^{(1,2)}\right)^{+} F^{\mathrm{lag}}(U_{i-1}^{(1)}, U_i^{(2)}) \\ & + \max\left(\alpha_{i-1}^{(2)} - \alpha_i^{(2)}, 0\right)\left(\beta_{i-1/2}^{(2,1)}\right)^{+} F^{\mathrm{lag}}(U_{i-1}^{(2)}, U_i^{(1)}).\end{aligned} \tag{49}$$

We assume that the flow evolves under initial uniform pressure and velocity conditions. Consequently, the pressures and velocity should remain constant during time evolution. We now check whether this property is satisfied or not at the discrete level by the scheme (47). Note that this basic property was fulfilled in [21] but not in [13].

In the following, we consider base fluxes for each phase that have the property, for any phase Σ_k.

If $u_i^{(k)}$ and $p_i^{(k)}$ are uniform on the stencil of the flux, then the pure fluid Euler scheme for phase Σ_k has the same uniform velocity and pressure after one time step.

A slight variant of this property was considered in [21]. We assume that it is possible to identify a wave structure, and a numerical contact discontinuity so that the Lagrangian flux can be defined

$$F^{\mathrm{lag}}(U, V) = F(U, V) - \sigma(U, V)U^*(U, V).$$

It is clear that if the velocity and pressure of the phase within one computational cell are in equilibrium, the Lagrangian flux is uniform. These two properties are obviously satisfied by the Godunov scheme, Roe scheme, HLLC scheme, etc.

Since the velocity and pressure of both phases are equal and uniform in space, the Lagrangian fluxes are constant and some flux indicator cancel (the velocity is assumed positive)

$$F^{\mathrm{lag}}(U_i^{(1)}, U_{i+1}^{(2)}) = F^{\mathrm{lag}}(U_i^{(2)}, U_{i+1}^{(1)}) = F^{\mathrm{lag}}(U_{i-1}^{(1)}, U_i^{(2)}) = F^{\mathrm{lag}}(U_{i-1}^{(2)}, U_i^{(1)}) = F^{\mathrm{lag},*}$$

then

$$\left(\beta_{i-1/2}^{(1,2)}\right)^{+} = \left(\beta_{i-1/2}^{(2,1)}\right)^{+} = \left(\beta_{i+1/2}^{(1,2)}\right)^{+} = \left(\beta_{i+1/2}^{(2,1)}\right)^{+} = 1$$

and

$$\left((\beta_{i-1/2}^{(1,2)}\right)^{-} = \left((\beta_{i-1/2}^{(2,1)}\right)^{-} = \left((\beta_{i+1/2}^{(1,2)}\right)^{-} = \left((\beta_{i+1/2}^{(2,1)}\right)^{-} = 0.$$

Owing to these simplifications the numerical fluxes and non-conservative terms reduce to

$$\mathscr{E}(XF)_{i+1/2} = F(U_i^{(1)})\Big(\max(\alpha_i^{(1)} - \alpha_{i+1}^{(1)}, 0) + \min(\alpha_i^{(1)}, \alpha_{i+1}^{(1)})\Big)$$

and

$$\mathscr{E}\left(F^{\text{lag}}\frac{\partial X}{\partial x}\right)_{i,\text{bound}} = F^{\text{lag},*}\Big(-\max\left(\alpha_{i-1}^{(1)}-\alpha_i^{(1)},0\right)+\max\left(\alpha_{i-1}^{(2)},\alpha_i^{(2)},0\right)\Big).$$

This reduces again to

$$\mathscr{E}(XF)_{i+1/2} = \alpha_i^{(1)}F(U_i^{(1)})$$

and

$$\mathscr{E}\left(F^{\text{lag}}\frac{\partial X}{\partial x}\right)_{i,\text{bound}} = (\alpha_i^{(1)}-\alpha_{i-1}^{(1)})F^{\text{lag},*}.$$

We now notice that $F(U_i^{(1)}) = F^{\text{lag},*}+\sigma U_i^{(1)}$ where $\sigma = u = \text{cst.}$ and denote $\lambda = \Delta t/\Delta x$. Thus the scheme (47) reduces to

$$(\alpha_i^{(1)}U_i^{(1)})^{n+1} = (\alpha_i^{(1)}U_i^{(1)})^n - \lambda u\Big((\alpha_i^{(1)}U_i^{(1)})^n - (\alpha_{i-1}^{(1)}U_{1,i-1}^{(1)})^n\Big). \tag{50}$$

We then drop superscript (1) and develop this equation for the various component of the vector $U = (1,\ \rho,\ \rho u,\ \rho E)^{\mathrm{T}}$. The volume fraction equation reads

$$(\alpha)_i^{n+1} = (\alpha)_i^n - \lambda u(\alpha_i^n - \alpha_{i-1}^n).$$

The mass conservation equation reads

$$(\alpha\rho)_i^{n+1} = (\alpha\rho)_i^n - \lambda u(\alpha_i^n\rho_i^n - \alpha_{i-1^n}\rho_{1,i-1}^n).$$

The momentum equation reads

$$(\alpha\rho u)_i^{n+1} = (\alpha\rho u)_i^n - \lambda u(\alpha_i^n\rho_i^n u_i^n - \alpha_{i-1}^n\rho_{i-1}^n u_{i-1}^n).$$

From these last two equations, it is obvious that

$$u_i^{n+1} = u_i^n.$$

The velocity does not change, in agreement with what was expected. Now we consider the energy equation

$$(\alpha\rho E)_i^{n+1} = (\alpha\rho E)_i^n - \lambda u(\alpha_i^n\rho_i^n E_i^n - \alpha_{i-1}^n\rho_{i-1}^n E_{i-1}^n).$$

Using the fact that the velocity does not evolve, we can eliminate the kinetic energy in the total energy. Thus, last equation can be rewritten in terms of internal energy

$$(\alpha\rho e)_i^{n+1} = (\alpha\rho e)_i^n - \lambda u(\alpha_i^n\rho_i^n e_i^n - \alpha_{i-1}^n\rho_{i-1}^n e_{i-1}^n).$$

We now introduce an equation of state (EOS). The stiffened gas EOS is able to describe gases, liquids and solids. It can be written as

$$\rho e = (P+\gamma P_\infty)/(\gamma-1)$$

with

$$\frac{1}{\gamma-1} = \frac{\alpha}{\gamma_1-1}+\frac{1-\alpha}{\gamma_2-1},$$

$$\frac{\gamma P_\infty}{\gamma-1}=\frac{\alpha P_\infty^{(1)}}{\gamma^{(1)}-1}+\frac{(1-\alpha)P_\infty^{(2)}}{\gamma^{(2)}-1},$$

where $\gamma^{(1)}, P_\infty^{(1)}$ (resp. $\gamma^{(2)}, P_\infty^{(2)}$) are the thermodynamical parameters of Σ_1 (resp. Σ_2).

Since the pressure is uniform at time level n, and since the parameters of the equation of state are constant too, a sufficient condition for the pressure to not evolve is

$$\alpha_i^{n+1}=\alpha_i^n-\lambda u(\alpha_i^n-\alpha_{i-1}^n)$$

which is in perfect agreement with the numerical update of the volume fraction obtained previously. The overall scheme satisfies perfectly the uniform pressure and velocity flow.

5.2. Flow in a uniform volume fraction field

In the particular case of two-phase flow with uniform volume fraction field, if we do not account for the relaxation terms, we expect that the fluids evolve freely, as they were evolving in a one-dimensional duct if they were alone. So we must recover the Godunov scheme for the Euler equations when the volume fraction is uniform.

Under uniform volume fraction condition we have

$$\mathscr{E}(XF)_{i+1/2}=\alpha_i^{(1)}F(U_i^{(1)},U_{i+1}^{(1)})$$

and

$$\mathscr{E}\left(F^{\text{lag}}\frac{\partial X}{\partial x}\right)_{i,\text{bound}}=0.$$

By eliminating $\alpha_i^{(1)}$ the scheme (47) reduces to

$$U_i^{(1),n+1}=U_i^{(1),n}-\lambda(F(U_i^{(1)},U_{i+1}^{(1)})-F(U_{i-1}^{(1)},U_i^{(1)})), \tag{51}$$

which is readily identified to the Godunov scheme.

6. Test problems

The method works for all tests of Refs. [21,24]. We have retained here the most important ones corresponding to various flow situation in shock tubes, the "water faucet test problem" of Ransom, a sedimentation problem and Rogue's test case to show that the method works for very different flow conditions.

6.1. Shock tubes with pure fluids and with mixtures

The tests are done with a uniform mesh of 200 cells. The materials are governed by the stiffened gas equation of state: $P=(\gamma-1)\rho e-\gamma P_\infty$. The parameters of the gas are $\gamma=1.4$ and $P_\infty=0$ while for the liquid they are $\gamma=4.4$ and $P_\infty=6\times10^8$ Pa.

The first shock tube involves a uniform volume fraction initial condition as shown in Fig. 9. The diaphragm separates two mixtures of equal volume fractions ($\alpha=0.5$). The left and right part of the shock tube contain fluids with a very strong pressure difference. The gas and liquid densities are 50 and 1000 kg/m^3, respectively, in the entire domain. The initial pressure in the high pressure chamber (left) is 10^9 and 10^5 Pa in the low pressure chamber (right).

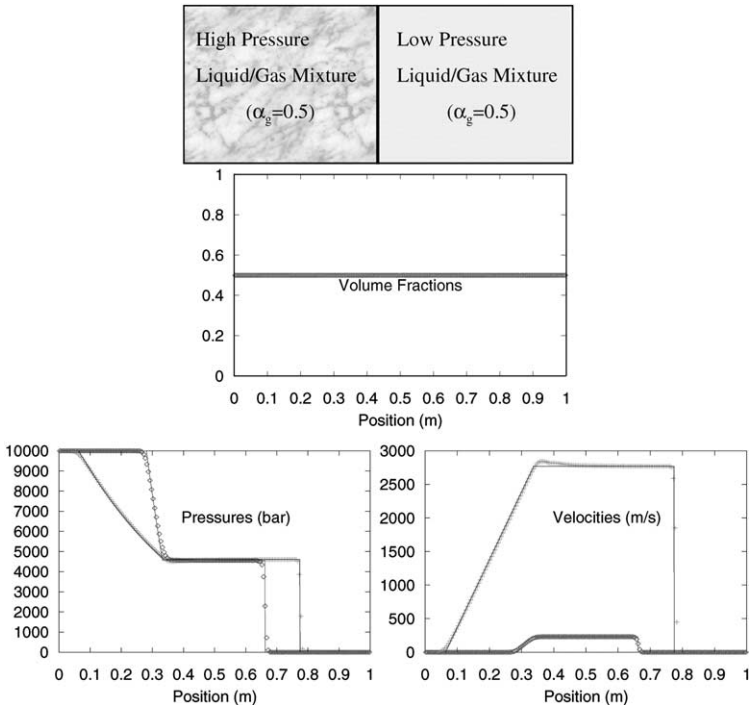

Fig. 9. Shock tube with two mixtures and uniform volume fraction. Second-order scheme of Section 4. No pressure and velocity relaxation procedures are used. Numerical solution with symbols. Exact solution with lines. The single phase behavior of the Euler equations is recovered.

We use the second-order variant of the method as described in Section 4. For this first run, we do not use any pressure and velocity relaxation procedure. The results are shown in Fig. 9, and the numerical solution of each fluid is compared to the exact one. The exact solution is obvious: each fluid evolves in a constant cross-section duct and is governed by the Euler equations. Excellent agreement is obtained.

Then, we run the same test with the relaxation procedure of Ref. [24]. Now the fluids have an infinite drag coefficient and the pressure relaxation is instantaneous. The results are shown in Fig. 10. The volume fraction varies across the rarefaction and shock waves. This behaviour is in perfect agreement with our previous results using a different scheme [21] and pressure and velocity relaxation procedures.

We now use the same initial conditions as in the previous test problem, but we change the initial volume fraction of the various fluids. An initial discontinuous profile is imposed. The left part of the shock tube contains the same liquid as before with an initial pressure of 2×10^8 Pa and an initial volume fraction of $\alpha_l = 1 - \epsilon(\epsilon = 10^{-6})$. Its right part is filled with a gas at 10^5 Pa with an initial volume fraction of $\alpha_g = 1 - \epsilon$. [3] This situation corresponds to a nearly pure liquid on the left high-pressure chamber and a nearly pure gas on the low pressure right chamber. We want to check if the method is again able to solve interface problem between nearly pure materials. The results are shown in Fig. 11 and are obtained with the second-order scheme combined with the pressure relaxation procedures of Ref. [24] as was done previously. We again obtain excellent agreement with the exact solution.

[3] This procedure is needed because we need to extract the conserved variable of each phase in order to compute the different needed fluxes. The result is not sensible to the choice of ϵ as we have checked numerically.

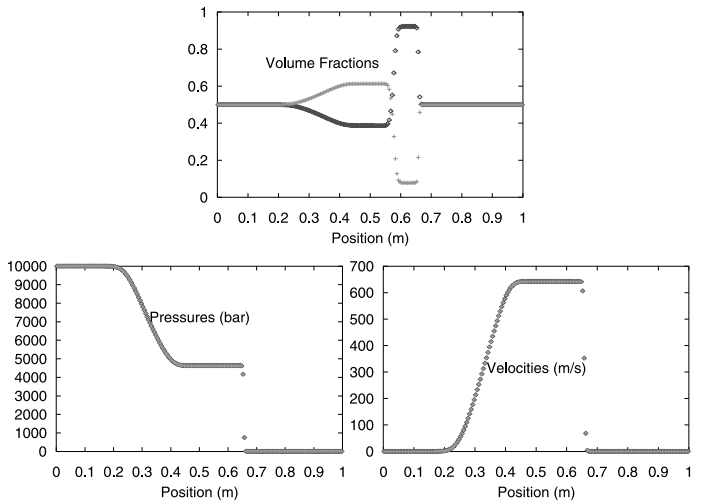

Fig. 10. Shock tube with well mixed materials of Fig. 9. Second-order scheme of Section 4. Pressure and velocity relaxation procedures of Ref. [24] are used.

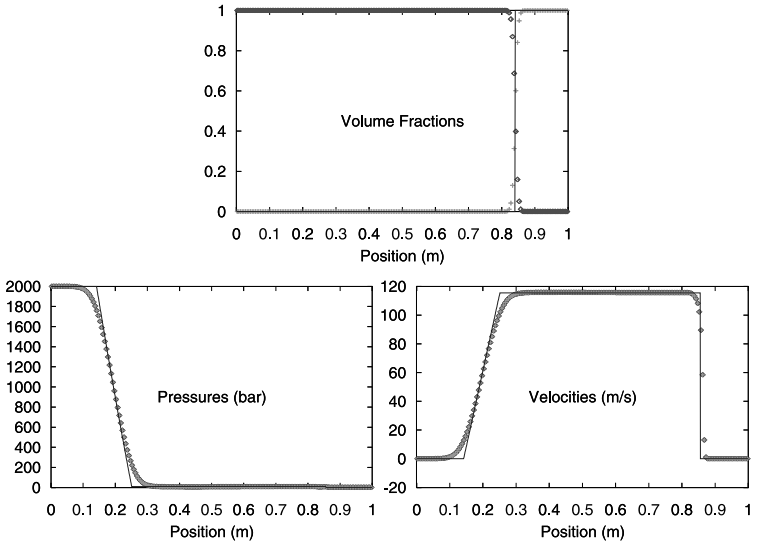

Fig. 11. Shock tube with interface separating nearly pure materials. Second-order scheme. Pressure and velocity relaxation procedures of Ref. [24] are used. Exact solution with lines, numerical solution with symbols.

We now redo the same test under the same initial conditions with a discontinuity in volume fraction. Contrarily to the previous calculations, we do not use any relaxation procedure as in [24], nor solve the ODE system (39). In other words, we take $\Lambda_i = 0$ in Eq. (35). This means that the two-phase control volume does not contain any internal interface. The only interfaces come from one of the cell boundary and its contribution to the evolution of the solution is controlled by (34) only. In absence of the relaxation terms (35), each fluid will retain its own pressure, velocity, etc, because there is no interaction between fluids. There is no drag force between the fluids, and of course no pressure relaxation. Hence, this test puts into

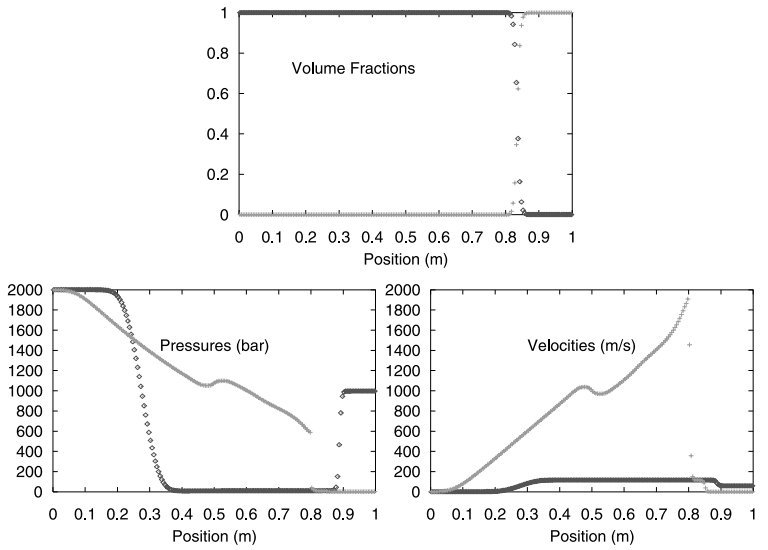

Fig. 12. Shock tube with interface separating nearly pure materials. Second-order scheme. No pressure and velocity relaxation procedures are used. The exact solution is shown in Fig. 11. Numerical solution with symbols. Each fluid has its own behavior, but at the interface, the pressure and velocity interface conditions are automatically fulfilled.

evidence the contribution of the non-conservative terms appearing in (34) only, that is the terms related to the interfaces that cross cell boundaries. The results are displayed in Fig. 12. As expected, the two fluids have very different pressure and velocities. They also have very different profiles because they do not have the same initial conditions, nor equation of state, and they evolve in different volumes. In the left part of the shock tube, the liquid is nearly pure and is expanded by a strong rarefaction wave. The solution of this rarefaction wave is in excellent agreement with the one obtained with a pure liquid on the left and a gas on the right. In the left part of the shock tube, the gas is expanded too. It accelerates near the interface because its volume varies in space and time. Indeed, the interface has a large velocity, and during its propagation, it is smeared by numerical diffusion. This numerical diffusion zone corresponds to a diverging nozzle where the gas is again expanded by geometrical effects.

We now consider the right part of the shock tube. A shock wave propagates into the gas due to the liquid–gas interface motion. The liquid existing in the right chamber in a negligible volume is moved too by a fast shock wave that is initiated in the stiff converging nozzle associated to the numerical diffusion zone.

The most interesting result of this test is that the coupling between the gas in the right part of the tube and the liquid on the left is achieved *perfectly* at the interface. The non-conservative terms (34) are able to restore the interface condition by the only fact that the volume fraction is discontinuous. The matching between the gas and the liquid variables at the interface is clearly shown on the magnified view of Fig. 13.

These results mean that the numerical model is able to deal with multiphase mixtures into non-equilibrium velocities as well as interface problems separating pure or nearly pure materials. Up to our knowledge, it is the first model able to deal with mixtures and interfaces under a unique formulation.

6.2. Ransom test problem

The water faucet problem consists of a vertical tube 2 m in length. The top has a fixed liquid velocity (10 m/s) and a liquid volume fraction of 0.8. The bottom of the tube is opened to atmospheric conditions. Initially, the tube is filled with a uniform column of liquid water at a velocity of 10 m/s surrounded by a gas

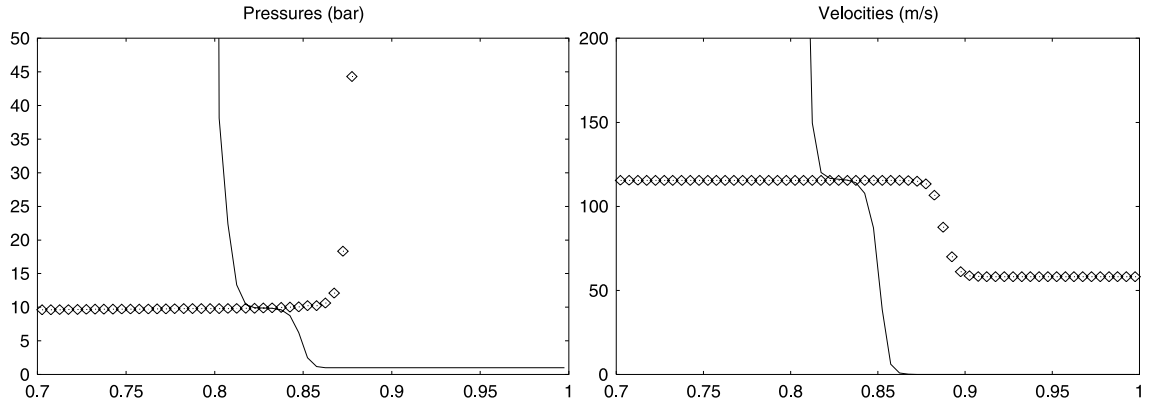

Fig. 13. Magnified view of the pressures and velocity profiles near the interface for the test of Fig. 12. Liquid solution with diamond symbols. Gas solution with lines. The interface conditions are automatically fulfilled.

at volume fraction of 0.2. From these initial conditions, gravity effects are considered and provoke a lengthening of the liquid jet. The gas and liquid are treated as compressible fluids with the same parameters and equation of state as for the liquid–gas shock tube test problem. Exact and numerical results are shown in Fig. 14.

The numerical solution shows an excellent agreement with the exact one even if the fluid compressibility necessitates the use of small time steps. Under mesh refinement, the solution converges to the exact one, contrarily to models involving pressure equality between phases and having a conditional domain of hyperbolicity.

6.3. Sedimentation case

We consider a tube filed with air and water. The tube is vertical and closed on top and bottom. Its length is 1 m. The mesh has 100 cells.

At initial time, the volume fraction of each phase is uniform and equal to 0.5. The initial velocity is 0 m/s, the initial pressure of both phase is 10^5 Pa. The air density is 1 kg/m^3, that of water is 1000 kg/m^3. At $t = 0$, we set up the gravity $g = 10\,\mathrm{m/s^{-2}}$, so that the heavy fluid falls down, and the light one moves up. At steady state, the tube should be filled with pure air in the upper half domain and with water on the remaining half

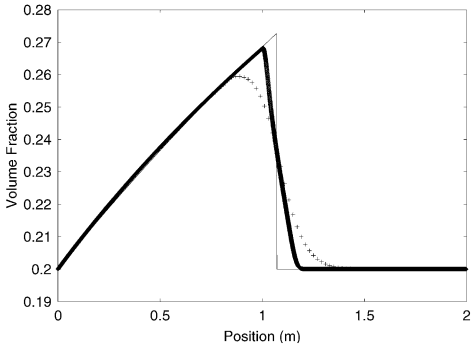

Fig. 14. Exact (full lines) and numerical solution (with 100 and 4000 cells) represented by symbols for the Ransom test problem.

tube. We show in Fig. 15 the volume fraction and pressure after at initial time and after 1.5 s. Here, we use the pressure equilibrium procedure. The results of Fig. 15 show that the method is able to separate fluids under body forces and fulfill interface conditions, starting from an ideal mixture.

6.4. Rogue test case

We consider here a vertical tube filled with air, see Fig. 16. In the middle, a bed of dense and small solid particles is settled. A shock wave propagates in the tube from the bottom. At some time, it crosses the bed

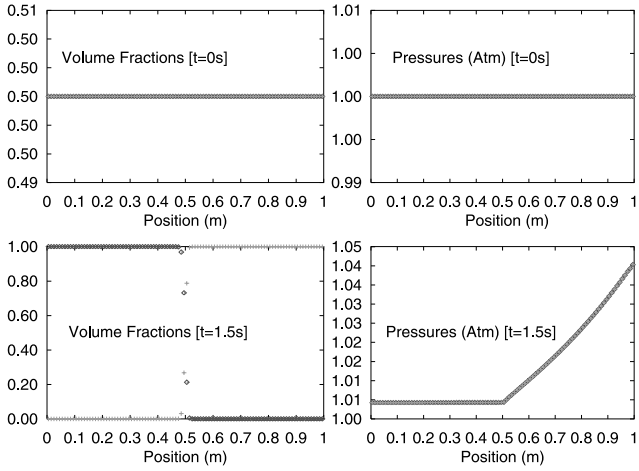

Fig. 15. Volume fractions and pressures at times $t = 0$ and $t = 1.5$ s for the sedimentation problem. ×, water; +, air.

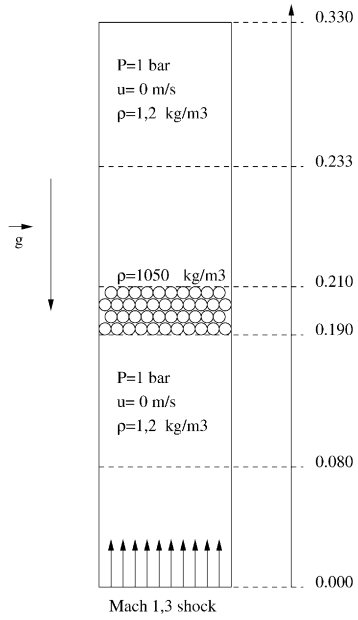

Fig. 16. Experimental setup, Rogue test case.

of particles, hence pressure disturbances and drag effects make the particle move. At the same time, the incident shock wave refracts, a transmitted wave propagates through the bed, and a reflected waves propagates backward. During the propagation of the transmitted wave, drag effects and volume fraction modification weaken the propagated shock, while the bed of particle moves.

To visualise the pressure evolution due to this very complex phenomena, two pressure gauges are installed, one before the particle bed, one after it. Their locations are 4.3 cm before the bottom of the particle bed and 11 cm after it. The bed thickness is 2 cm.

The particles are modelled as compressible particle, with the same parameters as for water. The drag effects on the particles are modelled with the drag force

$$F_{\mathrm{d}} = \frac{3}{4} C_{\mathrm{d}} \frac{\rho^{(1)}}{d_p} (1 - \alpha^{(1)}) |u^{(1)} - u^{(2)}| (u^{(1)} - u^{(2)}).$$

The various coefficients and parameters of the experimental setup are given in Table 3. The superscript (1) stands for the ambient gas and (2) for the particles.

There exists experimental results about this configuration, see [17,18]. No exact solution is known, of course. In Fig. 17, we have reported the experimental results for the pressure and computed ones. They are in good agreement.

The accuracy of the computed results could be improved by adding granular pressure and energy to the model. Doing this, the method would couple two more complicated systems than the Euler equations. This

Table 3
Parameters for the Rogue test case

Parameter	Value
Air preshock density	1.2 kg/m^3
Incident shock Mach number	1.3
Particle density	1050 kg/m^3
Particle diameter (d_p)	2 mm
Particle bed thickness	2 cm
Initial gas volume fraction in the bed	0.35
Drag coefficient (C_{d})	0.6

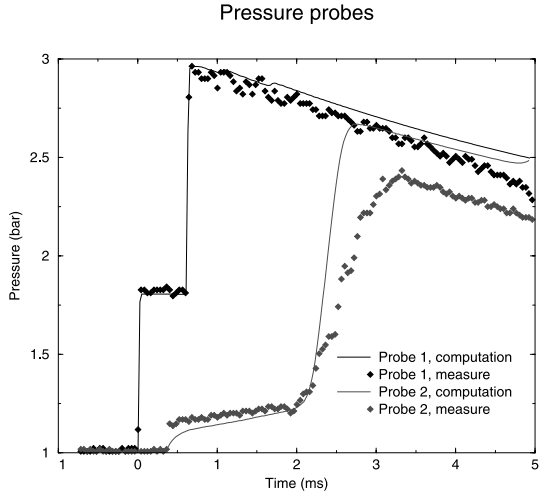

Fig. 17. Comparison between the experimental results and the computational ones.

type of work comes out of the scope of this paper. For addition of extra physics and hydrodynamics to the model, see [23].

7. Conclusions, perspectives

This paper describes a new philosophy for the modeling and numerical resolution of heterogeneous media. We have successfully applied it to interface problem and compressible multiphase mixtures. We believe that this concept may be applied to other physical problems of physical and mathematical importance.

The extension to multidimensional problems is possible [1], The only real modification, compared to the present developments, is about the coefficients $\mathscr{P}_{i\pm1/2}(\Sigma_p, \Sigma_q)$. They are defined as, for an interface between two computational cells, say between $]x_{i-1/2,j-1/2}, x_{i+1/2,j-1/2}[\times]y_{i-1/2,j-1/2}, y_{i+1/2,j-1/2}[$ and $]x_{i+1/2,j-1/2}, x_{i+3/2,j-1/2}[\times]y_{i-1/2,j-1/2}, y_{i+1/2,j-1/2}[$, that is $\{x_{i+1/2,j-1/2}\}\times]y_{i-1/2,j-1/2}, y_{i+1/2,j-1/2,}[$

$$\mathscr{P}_{i\pm1/2,j-1/2}(\Sigma_p, \Sigma_q) = \mathscr{E}\left(\int_{y_{i+1/2,j-1/2}}^{y_{i+1/2,j-1/2}} X(x_{i+1/2}, s)\, \mathrm{d}s \right),$$

which can be evaluated in the same way as in the present paper.

The problem of the relaxation coefficient is more interesting. In the one-dimensional situation, they are defined as the average number of internal interfaces. In the multidimensional case, using once more the same argument as here, they are the average area of internal bubbles in the x- and y-directions. It is interesting to note that the one-dimensional case can be interpreted in the same way. It is also noticeable that these quantities have already been introduced in the literature, see [6] for example.

Acknowledgements

The first author has been partially supported by CEA Cesta through the Laboratoire Correspondant du CEA, LRC No. 3. The second author has been partially supported by DGA/CEG Gramat and CEA/DAM Bruyeres le Chatel. He is particularly grateful to Gerard Baudin (DGA/CEG), Serge Gauthier and Francois Renaud (CEA Bruyeres le Chatel). This work could not have been done without the invaluable help of Jacques Massoni, Ashwin Chinnayya and Olivier LeMetayer of Polytech Marseille. The computations of Section 6.4 have been done by M. Papin (Mathematiques Appliquées de Bordeaux and Cea Cesta). We gratefully acknowledge them. The critical comments of Herve Guillard (INRIA Sophia Antipolis) and Smadar Karni (U. of Michigan, Ann Harbor) have been very stimulating and are acknowledged.

Appendix A. Proof of the Lax–Wendroff theorem

We show the following result.

Theorem A.1. *We consider the semi-discrete scheme* ((32)–(35)). *We define* W_Δ *by*

$$W_\Delta(x,t) = W_i^n \quad \text{if } (x,t) \in]x_{i-1/2}, x_{i+1/2}[\times[t_n, t_{n+1}[.$$

Thus, if we assume that, for $\Delta t/\Delta x$ *fixed,*

- *the sequence* W_Δ *is bounded in* $L^\infty(\mathbb{R}^+ \times \mathbb{R})$,
- *there exists* $W \in L^2(\mathbb{R}\times\mathbb{R}^+)_{\mathrm{loc}}$ *such that* $W_\Delta \to U$,

- *U is piecewise regular*,
- *the probability law of the flow is known and the relaxation coefficients remain bounded*,
- *if* $\mathscr{P}_{i+1/2}(\Sigma_p, \Sigma_q)$ *has the functional form* $\mathscr{P}_{i+1/2}(\Sigma_{\mathrm{p}}, \Sigma_q) = P_{pq}(\alpha_i^{(p)}, \alpha_{i+1}^{(q)})$ *with* P_{pq} *continuous and* $P_{pp}(\alpha, \alpha) = \alpha, P_{pq}(\alpha, \alpha) = 0$ *if* $p \neq q$.

Then, the limit solution is a weak solution of the problem, i.e., for any $\varphi \in C^1(\mathbb{R} \times \mathbb{R}^+)^4$,

$$\int_{\mathbb{R}\times\mathbb{R}^+} W_{(j)} \frac{\partial \varphi}{\partial t} + \mathscr{F}_{(j)}(W_{(j)}) \nabla \varphi - \int_{\mathbb{R}} W_{(j)}(x,0)\varphi(x,0) = \mathscr{E}\left(\int_{\mathbb{R}\times\mathbb{R}^+} (F(W_{(j)}) - \sigma W_{(j)}) \nabla X_{(j)} \varphi \right), \quad j = 1, 2.$$

Proof. Let $\varphi_i = \varphi(x_i)$. We have

$$\sum_i \Delta x \varphi_i \frac{\mathrm{d}W_i^{(j)}}{\mathrm{d}t} + \sum_i \varphi_i (\mathscr{E}(X_i F))_{i+1/2} - (\mathscr{E}(X_j F))_{i-1/2}) - \sum_i \varphi_i \left(\mathscr{E}\left(F^{\mathrm{lag}} \frac{\partial X}{\partial x} \right) \right)_{i+1/2} = 0. \tag{A.1}$$

The flux $\mathscr{E}(X_i F))_{i+1/2}$ is defined by (23) can be written in short as a sum of terms like $\beta \mathscr{P} F$. The term $(\mathscr{E}(F^{\mathrm{lag}}(\partial X/\partial x)))_{i+1/2}$ is the sum of "non-conservative" terms (25) and (26) and "relaxation" terms (27).

The non-conservative terms can be written as a sum of differences of terms of the type $\beta \mathscr{P} F^{\mathrm{lag}}$.

The difference between

$$\mathscr{S} = \sum_i \Delta x \varphi_i \frac{\mathrm{d}W_i^{(j)}}{\mathrm{d}t} + \sum_i \varphi_i (\mathscr{E}(X_i F))_{i+1/2} - (\mathscr{E}(X_j F))_{i-1/2}) - \sum_i \varphi_i (\mathscr{E}\left(F^{\mathrm{lag}} \frac{\partial X}{\partial x} \right))_{i+1/2}$$

and the same expression $\mathscr{S}^{\mathrm{exact}}$ obtained with the *exact* probabilities $\mathscr{P}^{\mathrm{exact}}$ is the sum of terms like $\beta(\mathscr{P} - \mathscr{P}^{\mathrm{exact}})F$ and $\beta(\mathscr{P} - \mathscr{P}^{\mathrm{exact}})F^{\mathrm{lag}}$. Then (A.1) can be rewritten as

$$0 = \mathscr{S}^{\mathrm{exact}} + \mathscr{S} - \mathscr{S}^{\mathrm{exact}}.$$

(I) We first show that

$$\mathscr{S}^{\mathrm{exact}} \to \int_{\mathbb{R}\times\mathbb{R}^+} W_{(j)} \frac{\partial \varphi}{\partial t} + \mathscr{F}_{(j)}(W_{(j)}) \nabla \varphi - \int_{\mathbb{R}} W_{(j)}(x,0)\varphi(x,0) - \mathscr{E}\left(\int_{\mathbb{R}\times\mathbb{R}^+} (F(W_{(j)}) - \sigma W_{(j)}) \nabla X_{(j)} \varphi \right)$$

for the Godunov flux.

Recalling that

$$(\mathscr{E}(X_{(j)} F))_{i+1/2} - (\mathscr{E}(X_{(j)} F))_{i-1/2}) - \sum_i \left(\mathscr{E}\left(F^{\mathrm{lag}} \frac{\partial X}{\partial x} \right) \right)_{i+1/2}$$

is the expectancy of

$$\sum_{l=2}^{N(\omega)-1} \int_{t_n}^{t+s} \int_{\xi_l + s\ \sigma(U_i^l, U_i^{l-1})}^{\xi_{l+1}+s\ \sigma(U_i^l, U_i^{l+1})} X \left(\frac{\partial U}{\partial t} + \frac{\partial F}{\partial x} \right) \mathrm{d}x\, \mathrm{d}t + \int_{CBB'} X \left(\frac{\partial U}{\partial t} + \frac{\partial F}{\partial x} \right) \mathrm{d}x\, \mathrm{d}t,$$

see Eq. (18) and Section 2.2, and since φ does not depend on ω, the index of the realization, we see that

$$\sum_i \varphi_i (\mathscr{E}(X_{(j)} F))_{i+1/2} - (\mathscr{E}(X_{(j)} F))_{i-1/2}) - \sum_i \varphi_i (\mathscr{E}\left(F^{\mathrm{lag}} \frac{\partial X}{\partial x} \right))_{i+1/2}$$

is the expectation of

$$\sum_{l=2}^{N(\omega)-1}\int_{t_n}^{t+s}\int_{\xi_l+s\ \sigma(U_i^{l-1},U_i^l)}^{\xi_{l+1}+s\sigma(U_i^l,U_i^{l+1})}\varphi_i X\left(\frac{\partial U}{\partial t}+\frac{\partial F}{\partial x}\right)\mathrm{d}x\,\mathrm{d}t+\int_{CBB'}\varphi_i X\left(\frac{\partial U}{\partial t}+\frac{\partial F}{\partial x}\right)\mathrm{d}x\,\mathrm{d}t.$$

Similarly, $\varphi_i(\mathrm{d}W_i^{(j)}/\mathrm{d}t)$ is the expectancy of $\varphi_i(\mathrm{d}XU/\mathrm{d}t)$, so that grouping the terms, we get that (A.1) is the expectancy of

$$\sum_i \Delta x\varphi_i\frac{dU_i^{(j)}}{dt}+\sum_{l=2}^{N(\omega)-1}\int_{t_n}^{t+s}\int_{\xi_l+s\ \sigma(U_i^{l-1},U_i^l)}^{\xi_{l+1}+s\ \sigma(U_i^l,U_i^{l+1})}\varphi_i X\left(\frac{\partial U}{\partial t}+\frac{\partial F}{\partial x}\right)\mathrm{d}x\,\mathrm{d}t+\int_{CBB'}\varphi_i X\left(\frac{\partial U}{\partial t}+\frac{\partial F}{\partial x}\right)\mathrm{d}x\,\mathrm{d}t.$$

Now the index ω is *fixed*, so using the classical arguments of the Lax–Wendroff theorem, and integrating in time, we see that, provided the probability law of the flow is known, we have

$$\mathscr{S}^{\mathrm{exact}}\to\int_{\mathbb{R}\times\mathbb{R}^+}W_{(j)}\frac{\partial\varphi}{\partial t}+\mathscr{F}_{(j)}(W_{(j)})\nabla\varphi-\int_{\mathbb{R}}W_{(j)}(x,0)\varphi(x,0)-\mathscr{E}\left(\int_{\mathbb{R}\times\mathbb{R}^+}(F(W_{(j)})-\sigma W_{(j)})\nabla X_j\varphi\right).$$

(II) Then we consider the remaining terms $\mathscr{S}-\mathscr{S}^{\mathrm{exact}}$ and show that

$$\mathscr{S}-\mathscr{S}^{\mathrm{exact}}\to 0.$$

As previously noted, they are sums of terms like

$$\varphi_i\Big(\{\beta(\mathscr{P}-\mathscr{P}^{\mathrm{exact}})F\}_{i+1/2}-\{\beta(\mathscr{P}-\mathscr{P}^{\mathrm{exact}})F\}_{i+1/2}\Big)$$

and

$$\varphi_i\Big(\{\beta(\mathscr{P}-\mathscr{P}^{\mathrm{exact}})F^{\mathrm{lag}}\}_{i+1/2}-\{\beta(\mathscr{P}-\mathscr{P}^{\mathrm{exact}})F^{\mathrm{lag}}\}_{i-1/2}\Big).$$

These terms are difference terms, so the same arguments as for the classical Lax–Wendroff theorem also apply. We note that almost every where, under the assumptions of Theorem A.1, that

$$\{\beta(\mathscr{P}-\mathscr{P}^{\mathrm{exact}})F\}_{i+1/2}\to 0$$

because $\mathscr{P}-\mathscr{P}^{\mathrm{exact}}\to 0$ almost everywhere.

(III) The relaxation terms contribute to

$$\sum_i\Delta x\varphi_i\Lambda_i\Big(F^{\mathrm{lag}}(U_i^{(2)},U_i^{(1)})-F^{\mathrm{lag}}(U_i^{(1)},U_i^{(2)})\Big).$$

Since U is bounded and since U is almost everywhere regular, we have

$$F^{\mathrm{lag}}(U_i^{(2)},U_i^{(1)})-F^{\mathrm{lag}}(U_i^{(1)},U_i^{(2)})\to 0$$

almost everywhere. Thanks to the Lebesgue dominated convergence theorem, they contributes to zero in the limit of a mesh refinement. This ends the proof. □

If we assume now that the flux F is only consistent with the continuous flux, and the same for F^{lag}. The difference between

$$\sum_i\Delta x\varphi_i\frac{\mathrm{d}W_i^{(j)}}{\mathrm{d}t}+\sum_i\varphi_i\left(\mathscr{E}(X^{(j)}F)\right)_{i+1/2}-\left(\mathscr{E}(X_{(j)}F)\right)_{i-1/2})-\sum_i\varphi_i\left(\mathscr{E}\left(F^{\mathrm{lag}}\frac{\partial x}{\partial X}\right)\right)_{i+1/2}$$

and the same expression with the Godunov flux is the sum of differences like

$$\varphi_i\Big(\{\beta\mathscr{P}(F-F^{\mathrm{God}})\}_{i+1/2}-\{\beta\mathscr{P}(F-F^{\mathrm{God}}\}_{i-1/2}\Big).$$

Then the same arguments as before applies. The justifies the scheme when the flux are not the Godunov scheme.

Similarly, the theorem can be extended to the second-order scheme because the basic ingredient we have used is the conservation of the non-averaged numerical scheme, and the continuity of the probabilities $\mathscr{P}$.

References

[1] R. Abgrall, L. Hallo, M. Papin, A numerical scheme for multidimensional multiphase compressible flows, Technical Report MAB 2002-34, Mathématiques Appliquées de Bordeaux, 2002.

[2] R. Abgrall, How to prevent pressure oscillations in multicomponent flow calculations: a quasi conservative approach, J. Comput. Phys. 125 (1996) 150–160.

[3] M.R. Baer, J.W. Nunziato, A two-phase mixture theory for the deflagration-to-detonation transition (DDT) in reactive granular materials, Int. J. Multiphase Flows 12 (1986) 861–889.

[4] J.B. Bzil, R. Menikoff, S.F. Son, A.K. Kapila, D.S. Steward, Two-phase modeling of a deflagration—to detonation transition in granular materials: a critical examination of modeling issues, Phys. Fluids 11 (2) (1999) 378–402.

[5] G. Dal Maso, P. Le Floch, F. Murat, Definition and weak stability of non-conservative products, J. Math. Pures Appl. 74 (1995) 483.

[6] J.-M. Delhaye, Some issues related to the modelling of interfacial areas in gas–liquid flows I. The conceptual issues, C.R. Acad. Sci. II b (329) (2001) 397–410.

[7] D.A. Drew, S.L. Passman, Theory of Multicomponent fluids, Applied Mathematical Sciences, volume 135, Springer, New York, 1998.

[8] P. Embid, M. Baer, Mathematical analysis of a two-phase model for reactive granular material, Continuum Mech. Thermodyn. 4 (1992) 279.

[9] P. Embid, J. Hunter, A. Majda, Simplified asymptotic equations for the transition to detonation in reactive granular materials, SIAM J. Appl. Math. 52 (1992) 1199.

[10] S. Gavrilyuk, R. Saurel, A compressible multiphase flow model with microinertia, J. Comput. Phys. 175 (2002) 326–360.

[11] E. Godlewski, P.A. Raviart, Hyperbolic Systems of Conservation Laws, Applied Mathematical Sciences, vol. 118, Springer, Berlin, 1995.

[12] S.K. Godunov, A. Zabrodine, M. Ivanov, A. Kraiko, G. Prokopov, Résolution numérique des problèmes multidimensionnels de la dynamique des gaz, Editions Mir, Moscow, 1979.

[13] K.A. Gonthier, J.M. Powers, A high-resolution numerical method for a two-phase model of deflagration-to-detonation transition, J. Comput. Phys. 163 (2000) 376–433.

[14] T.Y. Hou, P. Le Floch, Why non-conservative schemes converge to the wrong solution: error analysis, Math. Comp. 62 (1994) 497–530.

[15] A. Kapila, S. Son, J. Bdzil, R. Menikoff, D. Stewart, Two-phase modeling of DDT: structure of the velocity-relaxation zone, Phys. Fluids 9 (12) (1997) 3885–3897.

[16] J. Massoni, R. Saurel, G. Baudin, G. Demol, A mechanistic model for shock to detonation transition in solid energetic materials, Phys. Fluids 11 (3) (1999) 710–736.

[17] X. Rogue, Expériences et simulations d'écoulements diphasiques en tubes à choc, Ph.D. Thesis, Université de Provence, France, 1997.

[18] X. Rogue, G. Rodriguez, J.F. Haas, R. Saurel, Experimental and numerical investigation of the shock-induced fluidization of a particle bed, Shock Waves 8 (29–45) (1998).

[19] L. Sainsaulieu, Contribution à la modélisation mathématique et numérique des écoulements diphasiques constitués d'un nuage de particules dans un écoulement de gaz, Thèse d'Habilitation à Diriger des Recherches, Université Paris VI, 1995.

[20] L. Sainsaulieu, Travelling-wave solutions of convection–diffusion systems in nonconservation form, SIAM J. Math. Anal. 27 (5) (1996) 1286–1310.

[21] R. Saurel, R. Abgrall, A multiphase Godunov method for compressible multifluid and multiphase flows, J. Comput. Phys. 150 (1999) 425–467.

[22] R. Saurel, R. Abgrall, A simple method for compressible multifluid flows, SIAM J. Sci. Comp. 21 (3) (1999) 1115–1145.

[23] R. Saurel, S. Gavrilyuk, F. Renaud, A multiphase model with internal degree of freedom, application to shock–bubble interaction, J. Fluid. Mech. (2003) (accepted).
[24] R. Saurel, O. LeMetayer, A multiphase model for compressible flows with interfaces, shocks, detonation waves and cavitation, J. Fluid. Mech. 431 (2001) 239–271.
[25] E.F. Toro, Riemann Solvers and Numerical Methods for Fluid Dynamics, Springer, Berlin, 1997.
[26] I. Toumi, A weak formulation of Roe's approximate Riemann solver, J. Comput. Phys. 102 (1992) 360.